# Chemical and Biochemical Studies of Bacillithiol

by

Janelle P. N. Russell

Submitted in Partial Fulfillment of the Requirements

for the Degree of

Master of Science

in the

Chemistry

Program

YOUNGSTOWN STATE UNIVERSITY

August, 2012

Chemical and Biochemical Studies of Bacillithiol

Janelle P. N. Russell

I hereby release this thesis to the public. I understand that this thesis will be made available from the OhioLINK ETD Center and the Maag Library Circulation Desk for public access. I also authorize the University or other individuals to make copies of this thesis as needed for scholarly research.

Signature:

*Janelle P. N. Russell*, Student Date

Approvals:

*Dr. Nina V. Stourman*, Thesis Advisor Date

*Dr. Peter Norris*, Committee Member Date

*Dr. Michael A. Serra*, Committee Member Date

Peter J. Kasvinsky, Dean of School of Graduate Studies and Research Date

## Abstract

Bacillithiol (BSH), the α-anomeric glycoside of L-cysteinyl-D-glucosamine with L-malic acid, is the recently identified low-molecular-weight (LMW) thiol in low G + C content Gram-positive bacteria. Although BSH has not been fully characterized it is thought to have functions analogous to those of glutathione, the major LMW thiol present in eukaryotes. Glutathione is known to act as an antioxidant and functions to protect the cell against oxidation and other toxins. BSH has been shown to contribute to the detoxification of toxic compounds including some antibiotics. Since bacillithiol is not present in humans its metabolism presents novel targets for antibacterial drug therapies. An attempt was made to chemically synthesize BSH for its use in biochemical studies that would further elucidate its functions. The trichloroacetimidate method was employed for the introduction of the α-glycosidic bond linking D-glucosamine with an L-malic acid derivative. A cysteine derivative was prepared with a pentafluorophenyl group activating it for peptide bond formation with D-glucosamine. NMR and IR spectroscopy were used to confirm the synthesis of these compounds. Efforts made toward forming the peptide bond without the use of a peptide coupling reagent were unsuccessful.

## Acknowledgements

I would like to first acknowledge my advisor, Dr. Nina Stourman, for her guidance and support. She is a wonderful professor and advisor whom I greatly respect and admire. I cannot thank her enough. I would like to thank Dr. Peter Norris for his advice concerning organic synthesis and also for giving me space in his lab to perform my work. I also extend my gratitude to Dr. Michael Serra for being a part of my thesis committee. I would also like to acknowledge members of both Dr. Stourman's and Dr. Norris' lab groups for their support help in my work; especially to Lorna Ngo and Li Sui whom I have grown to think of as family.

I thank my parents for giving me an inquisitive mind and for showing me that it is never too late to go back to school. I thank my husband, Bryant Mitchell, for always supporting me and for believing that there is nothing I cannot do. Finally, I would like to extend my gratitude to the Youngstown State University Department of Chemistry for giving me the opportunity to teach and learn.

# Table of Contents

# List of Figures

# List of Equations

# List of Tables

# List of Abbreviations

| | |
|---|---|
| 1L-Ins-P | 1L-*myo*-inositol-1-phosphate |
| 4HNE | 4-hydroxy-2-nonenal |
| AcCys-GlcN-Ins | 1D-*myo*-inosityl-2-(*N*-acetyl-L-cysteinyl)-amido-2-deoxy-*α*-D-glucopyranoside or mycothiol |
| BSH | Bacillithiol |
| CAN | Ceric ammonium nitrate |
| CAT | Catalase |
| $CH_2Cl_2$ | methylene chloride or dichloromethane |
| Cys-GlcN-Ins | 1-*O*-[2-[[(2*R*)-2-amino-3-mercapto-1-oxopropyl]amino]-2-deoxy-α-D-myo-inositol |
| DMAP | 4-dimethylaminopyridine |
| DMF | Dimethyl formamide |
| EtOAc | Ethyl acetate |
| GCL | Glutamate-cysteine ligase |
| GlcNAc | *N*-acetylglucosamine |
| GlcNAc-Ins | 1-*O*-(2-acetemido-2-deoxy-α-D-glucopyranosyl)-D-*myo*-inositol |
| GlcNAc-Ins-P | 1-*O*-(2-acetemido-2-deoxy-α-D-glucopyranosyl)-D-*myo*-inositol-3-phosphate |
| GlcN-Ins | 1-*O*-(2-amino-2-deoxy-α-D-glucopyranosyl)-D-*myo*-inositol |
| GPX | Glutathione peroxidase |
| GS | Glutathione synthase |
| GSH | Glutathione |
| GSSG | Glutathione disulfide |
| GST | Glutathione transferase |
| LMW | Low-molecular-weight |
| MeOH | Methanol |
| MIC | Minimum inhibitory concentration |
| MSH | Mycothiol |
| NaOMe | Sodium methoxide |
| $PPh_3$ | Triphenylphosphine |
| RNS | Reactive nitrogen species |
| ROS | Reactive oxygen species |
| R-SH | Thiol |
| SH | Hydrogen sulfide |
| SOD | Superoxide dismutase |
| $Tf_2O$ | Trifluoromethanesulfonic anhydride |
| THF | Tetrahydrofuran |
| TMSOTf | Trimethylsilyl trifluoromethane sulfonate |
| UDP-GlcNAc | Uridine diphosphate *N*-acetylglucosamine |

# Chapter 1: Introduction

## *Thiols*

Sulfur is required by all organisms and plays a key role in major metabolic pathways. It has been shown that sulfur metabolic pathways are necessary for the mediation of virulence in many pathogenic bacteria, and can therefore be targeted for antimicrobial drug therapy (*1*). The thiol group (SH) is a biologically important sulfur containing functional group in both prokaryotic and eukaryotic cells. This highly reactive functional group has the ability to act as a nucleophile, form disulfide bonds, has redox properties and has an affinity for metal ions (*2*). Thiols are also easily oxidized by oxygen in the presence of heavy metals which leads to the production of reactive oxygen species (ROS) which can damage the cell. Some low-molecular-weight (LMW) thiols have structures that make them more resistant to autoxidation. They can function to protect the cell against oxidants and harmful electrophiles and help to maintain cellular redox homeostasis (*3*). Thiol-containing compounds have been investigated for their involvement in metabolic regulation, signal transduction, and the regulation of gene expression (*4*).

The simplest thiol, hydrogen sulfide ($H_2S$), can be found as a cofactor bound to many iron-sulfur proteins. In most iron-sulfur proteins iron is coordinated either to the sulfurs of cysteine residues from the polypeptide, or to inorganic sulfurs in prosthetic groups called iron-sulfur clusters. Iron-sulfur clusters are found in enzymes such as NADPH dehydrogenase and coenzyme Q – cytochrome c reductase and are best known for their participation in the oxidation-reduction reactions of the mitochondrial electron transport chain (*5*). Most other SH-groups in the cell are incorporated into the amino acid

cysteine (Fig. 1-1). Free cysteine is autoxidized rapidly in the presence of heavy metals leading to the production of toxic ROS. Cysteine found in high cellular concentrations is, therefore, mostly incorporated into proteins or other LMW thiols like glutathione (GSH), the predominant LMW thiol in humans (Fig. 1-2). The primary function of these LMW thiols is to participate in the detoxification of thiol-reactive oxygen byproducts and xenobiotics (*6*).

Under oxidative conditions protein thiols form disulfide bonds that stabilize tertiary structure and can also regulate protein function. In the reducing environment of the cytosol proteins are largely maintained in their reduced state, however, during times of oxidative stress, non-native disulfide bonds may form causing intermolecular protein cross-linking. This can impair protein function and ultimately result in cell death. Cellular LMW thiols are able to form reversible disulfide bonds with protein thiols protecting them from oxidative damage.

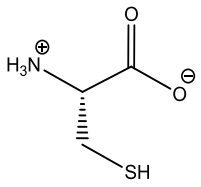


**Figure 1-1:** Structure of the amino acid cysteine

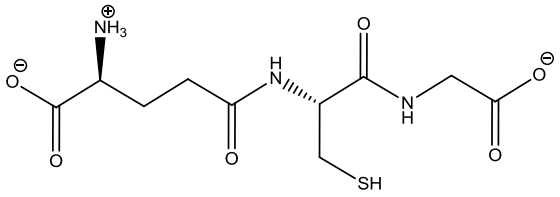


**Figure 1-2:** Structure of γ-L-glutamyl-L-cysteinylglycine or glutathione (GSH).

***Reactive Oxygen Species (ROS) and Reactive Nitrogen Species (RNS)***

Oxidants can be produced by normal cell functions as well as by environmental stressors. Reactive oxygen and reactive nitrogen species (ROS and RNS respectively) in the cell can have damaging effects on lipid membranes, nucleic acids, and proteins. Unrepaired, damaged DNA has been implicated as one of the major causes of aging; such damage can be induced by oxidation of nucleotides by ROS/RNS (*2*). ROS like hydrogen peroxide ($H_2O_2$), the superoxide anion ($O_2^{\bullet -}$), and the hydroxyl radical ($OH^{\bullet}$), can be generated as a result of incomplete electron transfer during the electron transport chain as well as through the oxidation of thiols by $O_2$. $H_2O_2$, $O_2^{\bullet -}$, and the strong oxidant hypochloric acid are generated by host immune response to bacterial infection. In mitochondrial electron transport the quinone is reduced to the semiquinone free radical which reacts with oxygen to produce $O_2^{\bullet -}$. This $O_2^{\bullet -}$ can then be enzymatically converted to $H_2O_2$ and water by superoxide dismutase (SOD) (*7*). Reactions with $H_2O_2$, and $O_2^{\bullet -}$ may occur outside of sites from which they were produced since they have a longer life-time; therefore, they are a threat to the entire cell. Hydrogen peroxide can also be converted to the hydroxyl radical ($HO^{\bullet}$) via a one electron transfer by the superoxide anion in the presence of heavy metals; known as the Haber-Weis reaction (*8*). The hydroxyl radical is one of the most toxic reactive oxygen radicals and can oxidize any organic molecule near it when it is produced. Reactions with $HO^{\bullet}$ are diffusion limited since the radical has an intracellular half-life of only $10^{-9}$ seconds (*9*). It is thought to contribute to, or cause, many of the toxic processes in diseases like cancer, diabetes, quinone toxicity, and radiation injury (*10*). When $HO^{\bullet}$ is produced near a membrane it can oxidize its lipids starting a free radical chain reaction, called lipid peroxidation. This

damages the membrane and leads to the formation of toxic side products like 4-hydroxy-2-nonenal (4-HNE), a reactive aldehyde that can inactivate proteins (*10*). RNS are formed by a diffusion-controlled reaction between $O_2^{\bullet -}$ and nitrogen oxide (NO) to give the peroxynitrite anion ($ONOO^-$), a strong oxidant that can react directly with nucleophiles (*9*). Protonation of $ONOO^-$ produces the conjugate acid, peroxynitrous acid (ONOOH), which breaks down to form nitrogen dioxide ($NO_2$), and $HO^{\bullet}$ (*10*).

***Antioxidants***

In order to combat the problem of oxidative stress, aerobic organisms must have mechanisms that protect against oxidation. Both enzymatic and nonenzymatic antioxidants exist in aerobic cells that function to protect the cell against oxidative stress. Antioxidant enzymes like superoxide dismutases (SOD), catalases (CAT), and peroxidases catalyze reactions that convert harmful oxidants into less reactive products (*9*). The dismutation of $O_2^{\bullet -}$ into less reactive $H_2O_2$ and molecular oxygen is catalyzed by SOD (Eq. 1-1).

**Equation 1-1:** $2\ O_2^{\bullet -} + 2H^+ \xrightarrow{SOD} H_2O_2 + O_2$

$H_2O_2$ produced within the cell is detoxified by CATs and peroxidases. CATs form a catalytically efficient family of enzymes which react with $H_2O_2$ to form water and molecular oxygen as shown in equation 1-2 (*9*). Peroxidases catalyze the reduction of $H_2O_2$ using an electron donor which gets oxidized in the reaction (*11*).

**Equation 1-2:** $2\ H_2O_2 \xrightarrow{CAT} 2\ H_2O + O_2$

Some nonenzymatic molecules classified as antioxidants include tocopherols, quinones, bilirubin, steroids, and LMW thiols like cysteine and glutathione (*8*). LMW

thiols like GSH are more resistant to heavy metal-catalyzed autoxidation than free cysteine allowing them to act as antioxidant molecules in protecting the cell against ROS. During oxidative stress, the production of these thiol containing compounds increases (*7*). Most of these detoxification reactions involve the nucleophilic attack of the thiolate on an electrophile. Post-translational modifications, known as *S*-thiolation, serve as a method of protection for protein thiols, and also as a control mechanism for redox-sensing transcription factors. These modifications involve the formation of a mixed disulfide between protein thiols and LMW thiols (*12*). *S*-Thiolation of active site cysteine residues protects them from irreversible oxidation that can alter protein function.

***Glutathione (GSH)***

Glutathione is the major LMW thiol found in eukaryotes and some bacteria, and is lacking in archea, and many Gram-positive bacteria. It is mainly present in the cytosol in the approximate range of 1-10 mM (*13*). Several roles of GSH have been elucidated including antioxidant defense, redox homeostasis, xenobiotic metabolism, and regulation of the cell cycle and gene expression (*7*). Structurally, it is a tripeptide, containing glutamate, cysteine, and glycine (γ-L-glutamyl-L-cysteinylglycine), with an unusual peptide linkage between the amino group of cysteine and the γ-carboxyl of the glutamate side chain (*14*). The *de novo* biosynthesis of GSH (Eq. 1-3 and 1-4) is both constitutive and induced (*7*). The first enzyme of the GSH biosynthetic pathway is glutamate-cysteine ligase (GCL), also called γ-glutamylcysteine synthetase. GCL catalyzes the formation of an amide bond between the γ-carboxyl group of L-glutamate and the amino group of L-cysteine coupled with ATP hydrolysis as shown in equation 1-3. The subsequent addition of glycine to γ-L-glutamyl-L-cysteine is carried out by glutathione

synthase (GS), also called glutathione synthetase, in an ATP-dependent reaction shown in equation 1-4 (*10*).

**Equation 1-3:** L-glutamate + L-cysteine + ATP $\xrightarrow{GCL}$ γ-L-glutamyl-L-cysteine + ADP + $P_i$

**Equation 1-4:** γ-L-glutamyl-L-cysteine + ATP + glycine $\xrightarrow{GS}$ γ-L-glutamyl-L-cysteinyl-glycine + ADP + $P_i$

GCL catalyzes the rate-limiting step and is regulated by the availability of L-cysteine, feedback inhibition by GSH, and transcriptional and post-translational regulation (*15*).

It is known that intracellular GSH content changes when the cell is exposed to stress. The presence of heavy metals, exposure to ROS/RNS or compounds that produce them, high glucose concentrations, and other reactive biological products can cause a temporary increase in GSH content by elevating the rate of its synthesis (*7*). GSH reduces toxic compounds to less harmful products via conjugation reactions either directly or enzymatically. The reduction of $H_2O_2$ and lipid hydroperoxides by GSH is an enzymatic reaction catalyzed by a glutathione peroxidase (GPX) where GSH acts as the electron donor. The reduction of $H_2O_2$ catalyzed by GPX produces $H_2O$ and glutathione disulfide (GSSG), as shown in equation 1-5. A similar reaction occurs in the reduction of lipid hydroperoxides where the hydroperoxide (ROOH) is reduced to its corresponding alcohol as shown in equation 1-6 (*9*).

**Equation 1-5**: $H_2O_2 + 2\ GSH \xrightarrow{GPX} 2\ H_2O + GSSG$

**Equation 1-6**: $ROOH + 2\ GSH \xrightarrow{GPX} ROH + GSSG + 2\ H_2O$

The depletion of intracellular GSH can be an indicator of oxidative stress since it is consumed in conjugation reactions. The production of GSH will then increase to replenish the intracellular supply of GSH. This is accomplished either by *de novo* synthesis or through the enzymatic reduction of GSSG back to GSH; however, it is mainly replenished by *de novo* synthesis (*7*). The reduction of GSSG by NADPH is catalyzed by glutathione reductase as shown in equation 1-7.

**Equation 1-7**: $GSSG + NADPH + H^{+} \xrightarrow{\text{Glutathione reductase}} NADP^{+} + 2\ GSH$

Under normal conditions less than 1 % of total glutathione exists in its potentially toxic disulfide form. Although there is an increase in GSSG during oxidative stress this increase is relatively temporary due to its rapid reduction as well as an ATP-dependent transport mechanism that exports GSSG from the cell. GSSG can also conjugate with protein thiols resulting in a mixed disulfide in a nonenzymatic reaction (Eq. 1-8) (*7*).

**Equation 1-8:** $GSSG + \text{protein-SH} \rightleftharpoons \text{protein-SSG} + GSH$

Mixed disulfides exchange with protein thiols to produce protein disulfides. GSH can form conjugates with electrophiles both enzymatically and nonenzymatically; an important function in xenobiotic metabolism. Nonenzymatic conjugation can occur if the electrophile is very reactive; however, most cases require a glutathione transferase (GST) (*7*). GSTs make up a superfamily of enzymes that catalyze the conjugation of GSH to an electron-deficient substrate, forming a GSH-*S*-conjugate (*16*). GSTs are dimers with each monomer containing at least two binding sites; a GSH binding site and a xenobiotic binding site. While the GSH binding site is very specific for GSH, the xenobiotic binding site is less specific; therefore, it is able to bind a variety of different toxins (*17*).

Further degradation of the GSH-*S*-conjugate is catalyzed by peptidases and an acetyl-CoA-dependent *N*-acetyltransferase. The glutamic acid and glycine residues are first cleaved by peptidases to give a cysteine-*S*-conjugate. The cysteine-*S*-conjugate is then acetylated to form a mercapturic acid derivative which is excreted from the cell (*3*).

***Mycothiol (MSH)***

Mycothiol (MSH) is the major LMW thiol in the high G + C content Gram-positive Actinobacteria, including *Mycobacterium* and *Streptomyces*. MSH is not found in eukaryotes or other bacteria. MSH, 1-D-*myo*-inosityl-2-(*N*-acetyl-L-cysteinyl)-amido-2-deoxy-*α*-D-glucopyranoside (AcCys-GlcN-Ins), has analogous functions to GSH although it differs in structure (Fig. 1-3). MSH is autoxidized 30 times slower than cysteine and seven times slower than GSH (*1*).

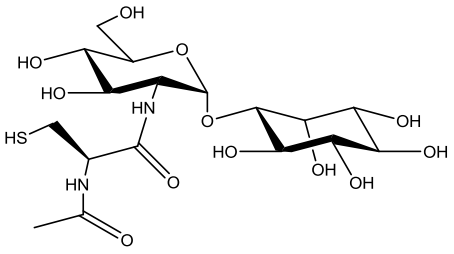


**Figure 1-3:** Structure of Mycothiol (MSH); 1-D-*myo*-inosityl-2-(*N*-acetyl-L-cysteinyl)-amido-2-deoxy-*α*-D-glucopyranoside (AcCys-GlcN-Ins).

Since MSH has detoxifying and antioxidant properties, and is not found in humans, its biosynthetic and metabolic pathways are important in the studies of antibiotic drug therapy (1). *M. tuberculosis,* the causative agent of tuberculosis, has especially high levels of MSH. It is able to survive and replicate in the oxidative, nutrient poor environment of the host macrophage and has become increasingly resistant to antibiotic

drugs. Antibacterial drugs, such as cerulenin, rifampin, and streptomycin, as well as other thiol-reactive agents are detoxified by MSH-dependent enzymes (*1*). *M. smegmatis* mutants lacking the genes that encode MSH biosynthetic enzymes show an increased sensitivity to oxidative stress, antibiotics, and alkylating agents (*1*). This increased sensitivity suggests the involvement of MSH, alone or along with MSH-dependent enzymes, in the protection of mycobacterium from oxidants and other toxins.

The biosynthesis of MSH, shown in Figure 1-4, requires five enzymes, MshA, MshA2, MshB, MshC, and MshD, and begins with the precursor 1-L-*myo*-inositol-1-phosphate (1L-Ins-1P). 1L-Ins-P is produced from glucose-6-phosphate by inositol phosphate synthase (Ino1). The first enzyme in the MSH biosynthetic pathway, MshA, is a glycosyltransferase. MshA catalyzes the addition of *N*-acetylglucosamine (GlcNAc) from uridine diphosphate *N*-acetylglucosamine (UDP-GlcNAc) to 1L-Ins-1P to produce 1-*O*-(2-acetemido-2-deoxy-α-D-glucopyranosyl)-D-*myo*-inositol-3-phosphate (GlcNAc-Ins-P). The GlcNAc-Ins-P intermediate is then dephosphorylated by the action of the MshA2 phosphatase. The next enzyme, MshB, is a divalent metalloprotein which deacetylates 1-*O*-(2-acetamido-2-deoxy-α-D-glucopyranosyl)-D-*myo*-inositol (GlcNAc-Ins) forming 1-*O*-(2-amino-2-deoxy-α-D-glucopyranosyl)-D-*myo*-inositol (GlcN-Ins) (*18*). Mutants that do not produce MshB are still able to synthesize MSH, although in decreased levels, suggesting that alternate deacetylases may compensate for the loss of MshB activity (*1*). The ligation of L-cysteine with GlcN-Ins is catalyzed by MshC in an ATP-dependent reaction to produce 1-*O*-[2-[[(2*R*)-2-amino-3-mercapto-1-oxopropyl]amino]-2-deoxy-α-D-myo-inositol (Cys-GlcN-Ins). The final enzyme, MshD, catalyzes the acetylation of the cysteine moiety using acetyl-CoA to give the final

product, AcCys-GlcN-Ins, or MSH (*18*). MshD is required for the synthesis of MSH; in its absence there is a build-up of its Cys-GlcN-Ins precursor and other analogs like *N*-formyl-Cys-GlcN-Ins (fCys-GlcN-Ins) and *N*-succinyl-Cys-GlcN-Ins (succ-Cys-GlcN-Ins). These analogs are thought to serve as alternative thiols for maintaining a reducing cellular environment (*1*). This can be seen in mutants that lack MshD but are still resistant to peroxide-induced oxidative stress. These mutants, however, do not grow well under other stress conditions like acidic growth media. The production of MSH is vital for the survival of *M. tuberculosis* but is not essential for growth of *M. smegmatis* probably owing to a larger genome that allows it to synthesize alternative thiols (*1*).

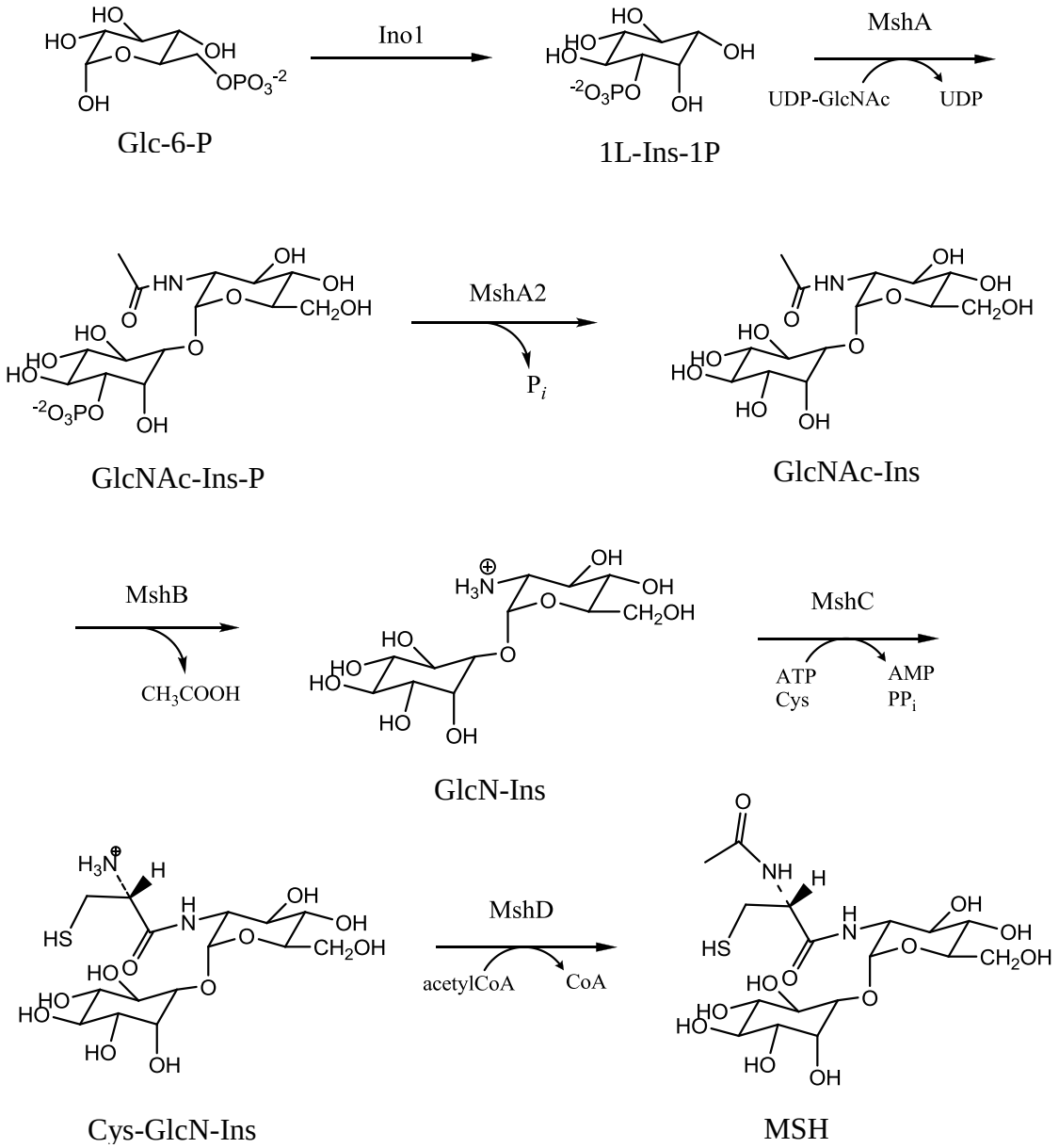


**Figure 1-4**: The MSH biosynthetic pathway adapted from Newton *et al* (*18*).

Like glutathione, MSH can react with toxins spontaneously and/or with MSH-dependent enzymes in the detoxification of toxic compounds like antibiotics. Many of the MSH-dependent enzymes are functionally analogous to GSH-dependent enzymes. Formaldehyde ($H_2CO$) reacts spontaneously with MSH. The product, *S*-hydroxymethylmycothiol, is a substrate for $NAD^+$/MSH-dependent formaldehyde dehydrogenase/nitrosothiol reductase (MscR). This enzyme converts the *S*-hydroxymethylmycothiol adduct into a MSH formate ester that is likely degraded to a carbonate ester, $CO_2$, and MSH by an aldehyde dehydrogenase (*19*). Mycothiol disulfide reductase (Mtr) is one of the key enzymes involved in maintaining levels of reduced MSH. Mtr is a member of the pyridine nucleotide-disulfide reductase superfamily of enzymes which includes glutathione disulfide reductase (*19*). MST, a member of the DinB family of thiol-*S*-transferases including GST, catalyzes the formation of MSH-toxin conjugates (*16*). MSH-*S*-conjugate amidase (Mca) then hydrolyzes the MSH-toxin conjugate into a mercapturic acid derivative containing the reactive moiety and GlcN-Ins. The mercapturic acid derivative is quickly exported out of the cell, and the GlcN-Ins is used in the future production of MSH (*1*). Mycobacterial mutants lacking Mca show an increased sensitivity to electrophiles, alkylating agents, and antibiotics like streptomycin (*3*). MSH can also contribute to antibiotic resistance through its influence on cellular redox status; either through its effect on the redox state of the entire cell or the cell wall which can affect its permeability (*1*).

***Bacillithiol (BSH)***

Bacillithiol **(**BSH) is the dominant LMW thiol recently identified in Firmicutes (low G + C content Gram-positive bacteria) including *Bacillus subtilis, Bacillus*

*anthracis*, and *Staphylococcus aureus* (*20*). It has analogous functions to GSH and MSH and is structurally similar to MSH (Fig. 1-5). Before BSH was identified, it was thought that *B. subtilis* use cysteine as its dominant antioxidant thiol and in some Firmicutes coenzyme-A (CoASH) has been shown to be the most abundant thiol. Cysteine by itself is not a suitable protective thiol due to its rapid autoxidation. Copper-catalyzed autoxidation of CoASH occurs at one-fourth the rate of GSH (*20*). However, the cysteine moiety is decarboxylated during the synthesis of CoASH and consequently cannot be regenerated. Therefore, CoASH is unfavorable as a protective thiol since it cannot serve as a reservoir for the regeneration of cysteine (*20*).

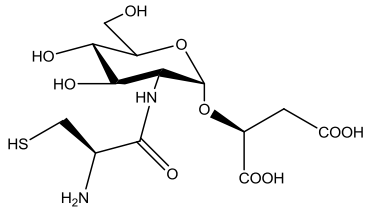


**Figure 1-5:** Structure of bacillithiol (BSH, or Cys-GlcN-Mal).

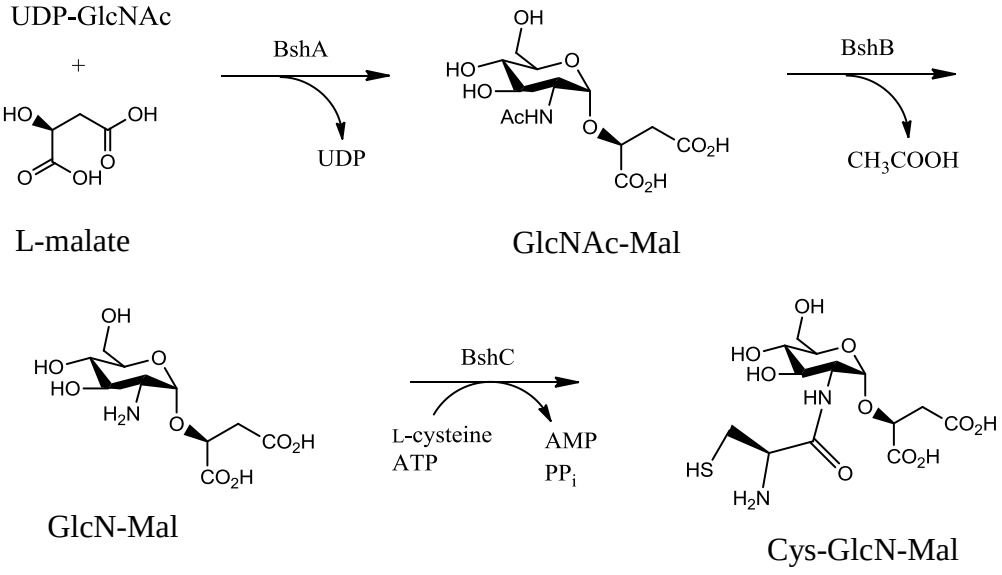


**Figure 1-6**: The biosynthetic pathway of bacillithiol adapted from Gaballa *et al* (*21*).

The genes and enzymes required for the biosynthesis of BSH have been identified (Fig. 1-6), and a synthetic pathway has been proposed based on similarities to MSH and verified through genetic and biochemical testing (*20*). The first enzyme in the BSH biosynthetic pathway, BshA, functions analogously to the MSH glycosyltransferase MshA. BshA, also a glycosyltransferase, catalyzes the glycosylation of L-malic acid, rather than 1L-Ins-1P in MSH, by the GlcNAc moiety of UDP-GlcNAc. The resulting intermediate, malyl-*N*-acetyl-D-glucosamine (GlcNAc-Mal) is then deacetylated by either of two deacetylases, BshB1 or BshB2. The final step in BSH synthesis, condensation of L-cystiene and GlcN-Mal, is catalyzed by a bacillithiol synthase, BshC, to give the final BSH product. All three enzyme activities are required for the synthesis of BSH. Deacetylation can be achieved by either BshB1 or BshB2. BSH is still synthesized if only one of these enzymes is present; however, it is not detected when both enzymes are eliminated (*21*). Candidates for the first two enzymes (BshA and BshB1/BshB2) were identified by bioinformatic analysis for their similarities to MshA and MshB, and have been characterized in *B. anthracis* (*22*). The gene that encodes BshC was identified through phylogenomic profiling using *bshA* as a query. It was identified as unknown protein YllA with no recognizable domains but is found in genomes that encode BshA, BshB1, and BshB2. The lack of homologs with BshC activity suggests that it is a previously uncharacterized enzyme (*21*).

Since BSH, like MSH, is not found in humans, and is present in several pathogens including *B. anthracis*, and *S. aureus*, it is also a possible target for antibacterial drug therapy (*20*). Although not yet fully elucidated, the detoxification pathways involving BSH seem to function analogously to those of GSH and MSH. BSH dependent

detoxification leads to the formation of *S*-conjugates (*3*). This was seen when *S. aureus* was treated with monobromobimane (mBBr), a fluorescent thiol reactive alkylating agent. A fluorescent BSH *S*-conjugate (BSmB) was produced which was then degraded by the activity of a bacillithiol conjugate amidase (Bca). Bca activity was evident by the production of Cys-bimane (CysmB) and increased intracellular levels of GlcN-Mal. The CysmB conjugate was converted to the mercapturic acid *N*-acetyl-Cys-bimane (AcCysmB) by an *N*-acetyltranferase. Both CysmB and AcCysmB were detected in the media, verifying their excretion from the cell (*3*). BSH null mutants have been shown to have increased sensitivity to a variety of environmental stressors including thiol reactive antibiotics (*3*).

Increased sensitivity to one antibiotic in particular, fosfomycin, has been observed when BSH is eliminated (*21*). Fosfomycin ((-)-cis-1,2-epoxypropyl phosphonic acid) is an epoxide-containing antibiotic that inactivates MurA (phosphoenolpyruvate UDP-*N*-acetylglucosamine-3-*O*-enolpyruvyl transferase), the enzyme that catalyzes the first committed step in peptidoglycan synthesis (*23*). Fosfomycin inhibits MurA by acting as an analog of its substrate, phosphoenolpyruvate. Resistance to fosfomycin involves enzyme dependent thiol conjugation with concomitant epoxide ring-opening (*24*). The BSH dependent enzyme FosB has been shown to contribute to fosfomycin resistance by catalyzing the conjugation of BSH with fosfomycin as shown in figure 1-7 (*21*). FosB is a BSH-dependent bacillithiol-*S*-transferase (BST) with analogous functions to the GSH- and MSH-dependent *S*-transferases in the detoxification of xenobiotics (*3*).

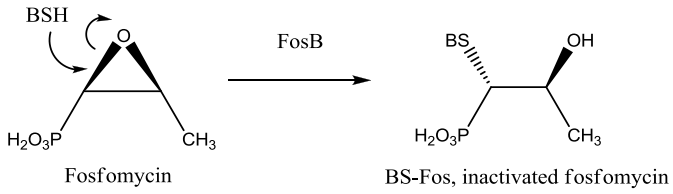


**Figure 1-7**: Mechanism of BSH-dependent inactivation of fosfomycin catalyzed by FosB adapted from Sharma *et al* (*25*).

Genes that encode FosB, thiol-*S*-tranferase fosfomycin resistance genes (*fosB*), have been detected in bacteria that produce BSH. *fosB* null mutants are equally sensitive to fosfomycin as are null mutants in BSH biosynthetic genes. Double mutants are no more sensitive to fosfomycin than single mutants. These findings suggest that the activity of FosB is dependent on BSH (*21*).

***Chemical synthesis of biological thiols***

Increasing resistance to antibacterial drug therapies has been observed in many pathogenic bacteria that produce MSH or BSH (*23*). Since LMW thiols have been shown to contribute to pathogenic virulence and antibiotic resistance, the metabolic and biosynthetic pathways are possible targets for new drug therapies. Obtaining these thiols in sufficient amounts for biological testing, however, has proven difficult. BSH is only found in intracellular quantities of 0.10 to 0.35 mM, and has been isolated from *Deinococcus radiodurans* as its bimane derivative in small quantities (approximately 50 µg per liter of cell culture) (*25*). Similarly, whole cell synthesis from *M. smegmatis* typically yields only 1 mg of MSH per liter of cell culture (*26*). Consequently, chemical methods for the complete synthesis of these thiols and their analogs are necessary to aid in their further characterization. A synthetic MSH analog, des-*myo*-inositol mycothiol, has been synthesized and was used to verify the activity of a mycobacterial-specific

reductase in *M. smegmatis* (*27*). This oxidized analog of mycothiol lacks *myo*-inositol; however, it is still recognized by some of the MSH-processing enzymes. Des-*myo*-inositol mycothiol has also been synthesized as its disulfide as a substrate for mycothiol reductase inhibitor assays (*26*).

Some of the major difficulties encountered when attempting to synthesize MSH are the α-glycosylation of D-*myo*-insoitol, the attachment of *N*-acetylcysteine by peptide bond formation, and deprotection. In 2004 the first total synthesis of mycothiol was reported by Lee and Rozassa (Fig. 1-16) (*28*). They introduced the α-glycosidic linkage through the coupling of the 1-OH of an acetylated D-*myo*-inositol acceptor (D-2,3,4,5,6-penta-*O*-acetyl-*myo*-inositol) with an acetylated azido trichloroacetimidate donor (*O*-(3,4,6-tri-*O*-acetyl)-2-azido-2-deoxy-*α*-*β*-D-glucopyranosyl trichloroacetimidate) (*28*). Trichoroacetimidate donors are one of the most common glycosyl donors used for the synthesis of *O*-glycosides (*29*). For trichloroacetimidate donors of 2-amino-2-deoxy sugars, non-participating groups, such as benzyl or azide, at C-2 contribute to the formation of the α-glycoside as the major product. This is anchimeric assistance (*30*). Other factors known to affect stereoselectivity are temperature and pressure, protecting groups, solvent, promoter, steric hinderence, and the nature of the leaving groups (*29*). Since trichloroacetimidates are best activated by strong acid catalysts (*29*), trimethylsilyl trifluoromethanesulfonate (TMSOTf) was used to promote glycosylation resulting in a 9:1 ratio of α to β isomers (*28*). The non-participating azide group was reduced using palladium on carbon (Pd/C) in the presence of HCl to give a protected amine hydrochloride. Peptide bond formation between a protected L-cysteine (*N*,*S*-diacetyl-L-cysteine) and the free amine of GlcN-Ins was facilitated by peptide coupling agents *O*-(7-

azabenzotriazol-1-yl)-*N*,*N*,*N*′,*N*′-tetramethyluronium-hexafluorophosphate (HATU) and 1-hydroxy-7-azabenzotriazole (HOAt), with collidine to give the protected MSH product. These coupling agents are used to increase reaction rate and yield, and to decrease racemization when forming amide bonds (*31*). Protected MSH was also obtained using carbodiimide coupling agents 1-Ethyl-3-(3-dimethylaminopropyl)-carbodiimide (EDC) and *N*,*N*′-dicyclohexylcarbodiimide (DCC); however, use of these reagents resulted in lower yields and significant epimerization of *N*-acetylcysteine. Finally, magnesium methoxide ($Mg(OMe)_2$) in methanol was used to selectively deacetylate the esters and thioesters of the protected molecule while leaving the amine group of cysteine acetylated. This deprotection step affords the desired MSH and MSSM products (Fig 1-8) (*28*).

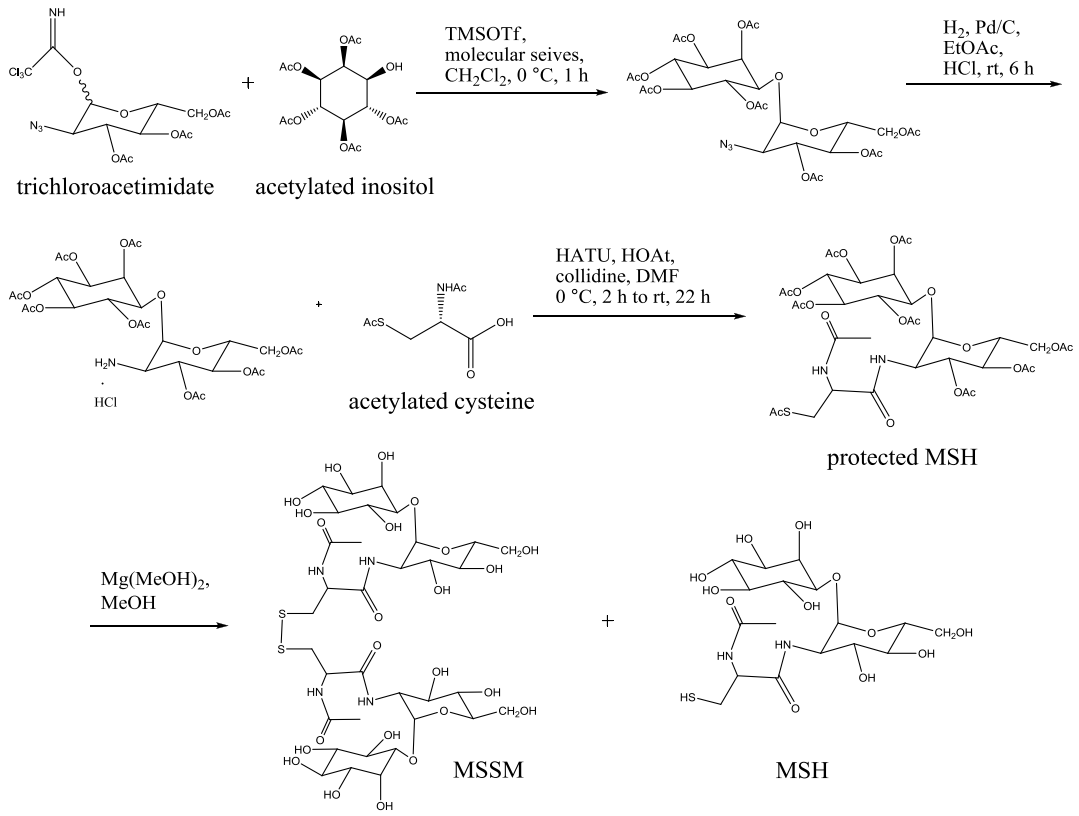


**Figure 1-8**: Total synthesis of MSH by Lee and Rozassa (28).

Since BSH is structurally similar to MSH, it is expected that some of the same methods could be employed in its synthesis. The chemical and chemoenzymatic synthesis of BSH and its biosynthetic intermediates, GlcNAc-Mal and GlcN-Mal, were reported in 2011 by Sharma *et al* (Fig. 1-9) (*25*). This synthetic BSH was used to verify that FosB functions as a bacillithiol-*S*-transferase, and that BSH is the preferred substrate for FosB. As in mycothiol synthesis, a trichloroacetimidate donor (2-azido-2-deoxy-3,4,6-tri-*O*-acetyl-α,β-D-glucopyranosyl trichloroacetimidate) was created to enable the formation of the α-glycosidic bond. The trichloroacetimidate donor then reacted with an L-malate acceptor, in which the carboxyl groups are protected by allyl esters, in the presence of the TMSOTf promoter. This reaction results in good α/β selectivity; giving a ratio of 96:4 (α:β) as determined by NMR (*25*). The azide group was then reduced via Staudinger reduction to the free amine. Protected BSH was formed by coupling a protected cysteinyl pentafluorophenyl ester with the free amine using 1-hydroxybenzotriazole (HOBt) as a peptide coupling reagent and racemization suppressor. A two-step deprotection strategy removes the allyl esters and the acetate protecting groups. The allyl esters are removed by catalytic tetra-*kis*(triphenylphosphine)palladium ($Pd(PPh_3)_4$) in the presence of excess imidazole. Acetate protecting groups are removed under mild Zemplen conditions to yield unprotected bacillithiol (*25*). Commercially available UDP-GlcNAc and L-malate were used as building blocks for the chemoenzymatic route. Recombinant BshA purified from *B. subtilis* was used to enzymatically catalyze the formation of the α-glycoside to give the unprotected D-GlcNAc-L-Mal intermediate. This intermediate was then converted to the deacetylated intermediate, D-GlcN-L-Mal, by recombinant *B. anthracis* BshB (*Ba*BshB) purified from *E. coli*. The addition of the cysteine residue was then

carried out by chemical coupling using HATU as the peptide coupling reagent (*25*). The chemoenzymatic route is shorter and more stereoselective and allows access to unprotected intermediates of the biosynthetic pathway. However, the UDP-GlcNAc is an expensive building block and this method must be carried out in a laboratory equipped for enzymatic synthesis.

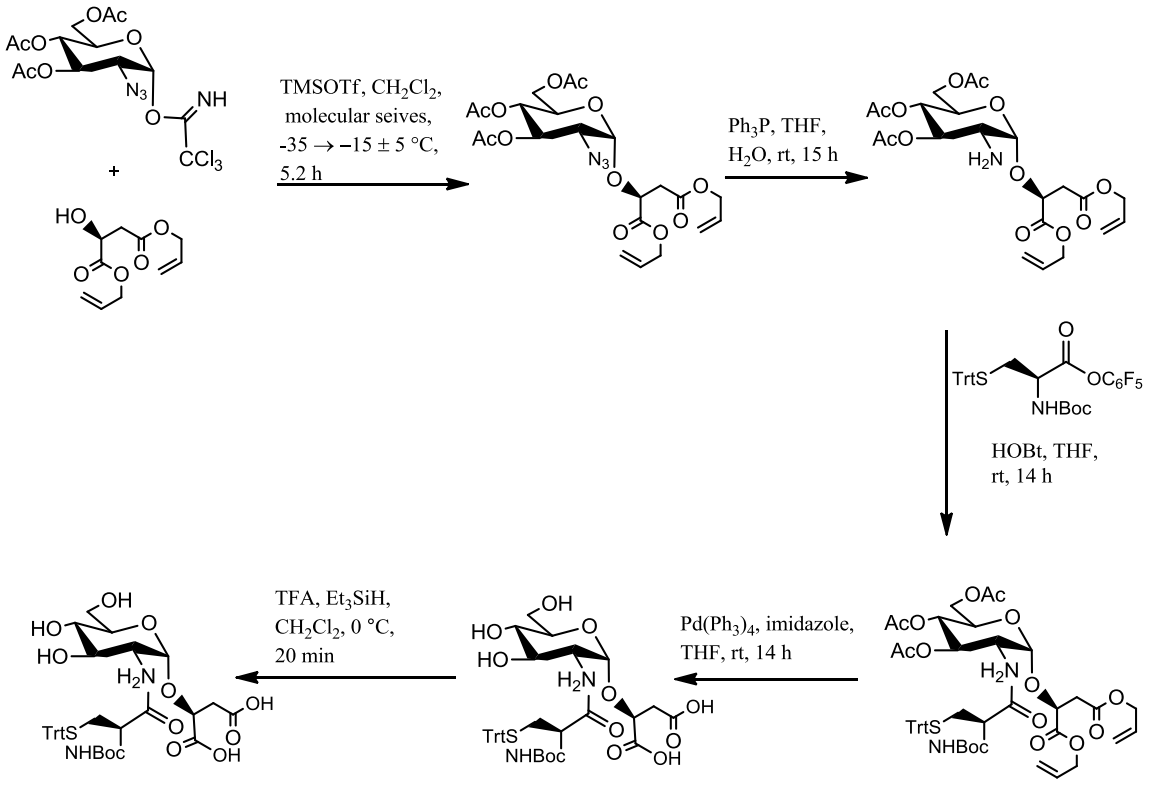


**Figure 1-9:** Chemical synthesis of BSH by Sharma *et al* (*25*).

***Statement of Purpose***

The known functions of BSH include the protection of bacteria against some antibiotics and other stress conditions. BSH is not present in humans, therefore, its metabolism could be targeted for antibacterial drug therapy. The objective of this study is to synthesize bacillithiol for the purpose of furthering its characterization.

The trichloroacetimidate method described by Rele *et al* (*32*) will be used to create a suitable glycosyl donor for the introduction of the α-glycosidic bond between D-glucosamine and L-malic acid. The addition of an azide moiety to the trichloroacetimidate at C-2 will be used to direct the synthesis of the α-anomer as the major product. Methods described by Sharma *et al* (*25*) will be employed for the production of L-malic acid and L-cysteine derivatives that are protected and activated for their linkage with the trichloroacetimidate. NMR and IR spectroscopy will be used to confirm the synthesis of these products. The MIC of fosfomycin in *B. subtilis* will be determined using the disc diffusion method (*35*).

# Chapter 2: Materials and Methods

## *Materials*

Acetic anhydride (anhydrous), acetonitrile, ceric ammonium nitrate, cesium carbonate, anhydrous pyridine, and anhydrous trimethylsilyl trifluoromethane sulfonate were obtained from Acros Organics (Pittsburgh, Pennsylvania). Bacteriological agar was purchased from Amresco (Solon, Ohio). Nutrient media was obtained from Himedia Laboratories (Mumbai, India). Anhydrous magnesium sulfate, potassium carbonate, sodium bicarbonate, sodium chloride, anhydrous sodium sulfate, and triethylamine were purchased from PharmCo-AAPER (Shelbyville, Kentucky). 4Å molecular sieves, allyl bromide, Boc-Cys(Trt)-OH, Celite, D-glucosamine hydrochloride, dimethyl malate, 4-dimethylaminopyridine, hydrazine acetate, sodium hydride (60 % dispersion in mineral oil), pentafluorophenyltrifluoroacetate, phosphomycin disodium salt, silica gel (200-400 mesh 60 Å), sodium azide, sodim methoxide, and trichloroacetonitrile were purchased from Sigma-Aldrich (St. Louis, Missouri). TLC plates (fluorescence UV 254) were obtained from Whatman (Kent, England). *Bacillus subtilis* cells were generously supplied by Dr. Gary Walker from the Department of Biology at Youngstown State University.

***Methods***

*General reaction scheme for the synthesis of bacillithiol.*

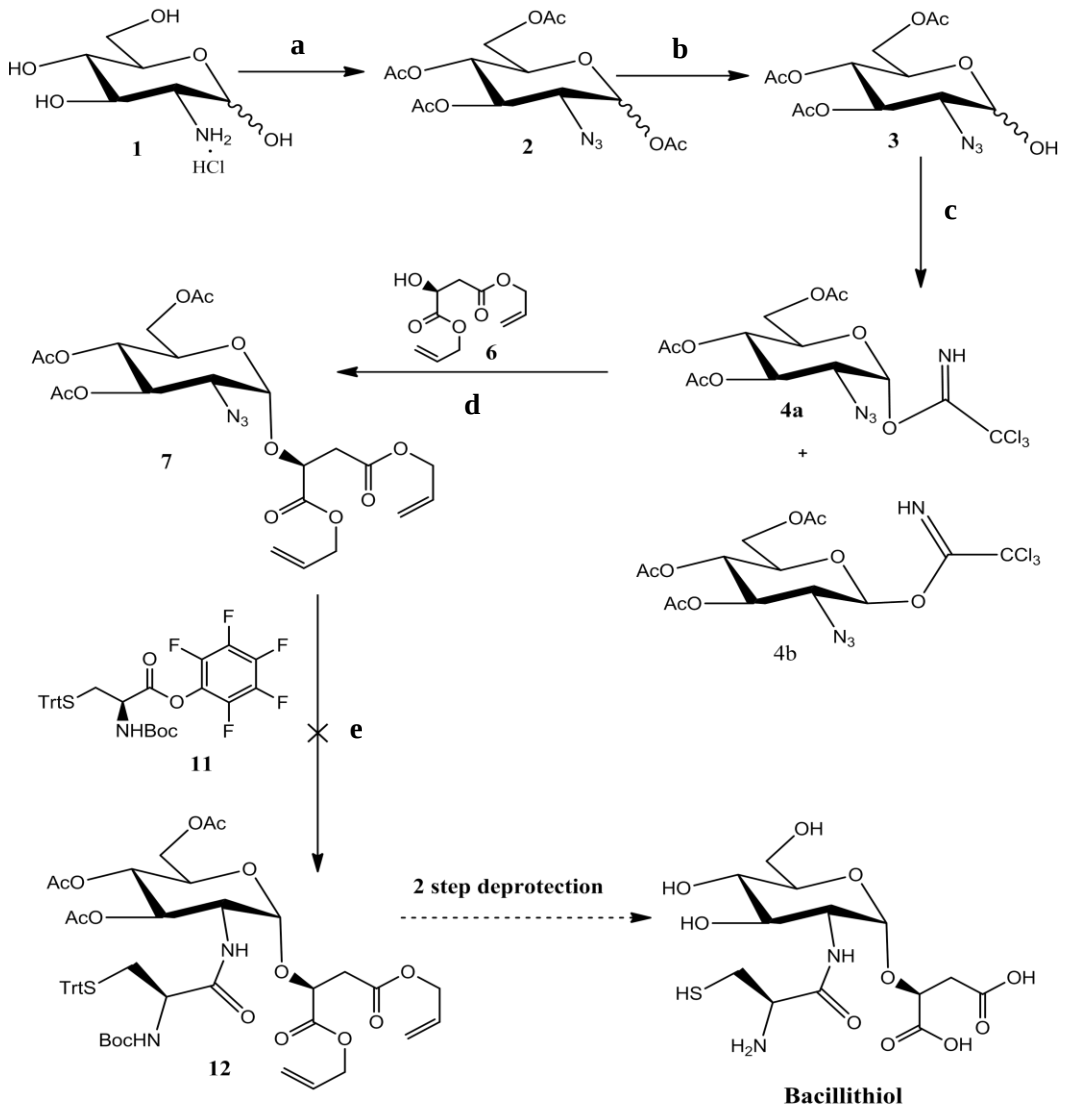


**Figure 2-1:** General reaction mechanism for the synthesis of BSH; reagents and conditions: (a) (1) $TfN_3$, MeOH, DMAP, 25 ºC, 18 h, (2) $Ac_2O$, pyridine, 0 ºC, 10 h; (b) $H_2NNH_2$ • AcOH, DMF, 0 to 25 ºC, 45 min; (c) NaH, $CCl_3CN$, dry $CH_2Cl_2$, rt, 3-5 h; (d) TMSOTf, dry $CH_2Cl_2$, 4Å molecular sieves, -35 to -15 ± 5 ºC, 5 h; (e) (1) $PPh_3$, THF, $H_2O$, 15 h, (2) DMF, $Et_3N$, cysteine pentafluorophenyl ester **11**, rt, 12 h.

*Synthesis of 2-azido-2-deoxy-3,4,6-tri-*O*-acetyl-α,β-D-glucopyranosyl acetate (**2**).*

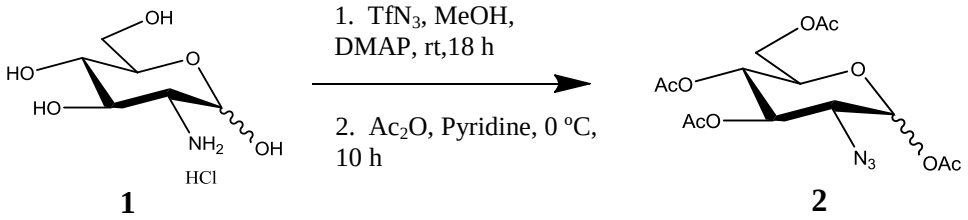


**Figure 2-2:** Synthesis of glucopyranosyl acetate (**2**).

Synthesis of trifluoromethanesulfonyl azide ($TfN_3$)

40 mL $H_2O$ and 38 mL $CH_2Cl_2$ were added to 14 g (0.22 mol) $NaN_3$ in a round bottom flask equipped with a nitrogen balloon. The reaction mixture was allowed to cool to 0 ºC and 7.5 mL dry $Tf_2O$ was added dropwise. After stirring for 2 h at 0 ºC, the ice was removed and the mixture was allowed to stir at room temperature for 15 minutes. The separated aqueous phase was extracted with 2 × 15 mL $CH_2Cl_2$. All organic fractions were combined and washed with cold saturated $NaHCO_3$ solution, washed with water, dried over anhydrous $MgSO_4$, and filtered through filter paper. This solution contained approximately 0.5 mol $TfN_3$ and was either used immediately or stored at -20 °C. IR spectroscopy was use to confirm the presence of the bound azide group as a sharp peak at 2153 $cm^{-1}$.

Azidation and acetylation of D-glucosamine

D-Glucosamine (**1**) (4.5 g, 0.021 mol) was dissolved in 175 mL MeOH in a three-necked round bottom flask. A 0.5 M solution of NaOMe in MeOH was prepared and added (40 mL) to the reaction mixture. After stirring 30 min at room temperature, 2.5 g DMAP was added, and the mixture was diluted with an additional 50 mL MeOH. The recently prepared $TfN_3$ solution was added via cannula under positive $N_2$ pressure. The reaction mixture was allowed to stir at room temperature under inert atmosphere for 18 h. The solvent was removed *in vacuo*. The resulting paste was acetylated via the addition of 175 mL anhydrous pyridine and 60 mL (0.63 mol) dry acetic anhydride added in 10 mL aliquots at 0 ºC for 10 h. The sticky dark brown reaction mixture was then coevaporated with toluene (3 × 75 mL) to remove pyridine. The product was purified by flash chromatography (3:1 hexane/EtOAc) to yield an α/β mixture of acetate **2** (4.56 g, 0.012 mol, 59% yield) as a light yellow gel.

$^1$H NMR (400 Mz $CDCl_3$): δ 6.32 (d,1H, H-1α, *J* = 3.68 Hz), 5.58 (d, 1H, H-1β, *J* = 8.56 Hz), 5.50 (dd, 1H, H-3, *J* = 9.52, 10.36 Hz), 5.15 - 5.04 (m, 3H), 4.34 - 4.29 (m, 2H), 4.16 - 4.05 (m, 4H), 3.84 - 3.80 (m, 1H), 3.40 - 3.64 (m, 2H, H-2), 2.21 (s, 3H), 2.21 (s, 3H), 2.12 (s, 3H), 2.11 (s, 3H), 2.10 (s, 6H), 2.06 (s, 3H), 2.04 (s, 3H).

*Synthesis of 2-azido-2-deoxy-3,4,6-tri-*O*-acetyl-α,β-D-glucopyranoside (**3**).*

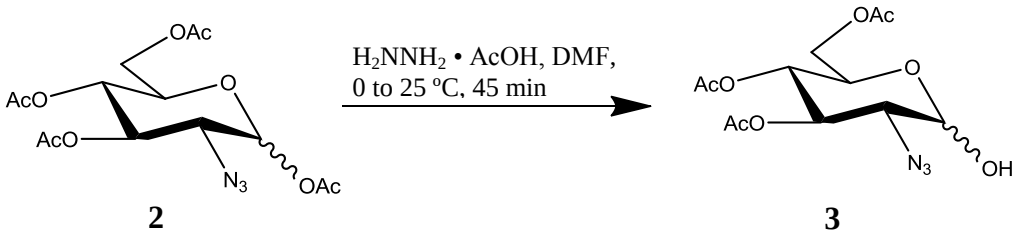


**2** **3**

**Figure 2-3:** Synthesis of glucopyranoside **3**.

2.5 equivalents (0.29 g, 3.14 mmol) of solid hydrazine acetate was added to an ice cooled solution of **2** (0.47 g, 1.25 mmol) dissolved in 4 mL anhydrous DMF. The ice bath was removed and the reaction mixture was allowed to stir at room temperature to completion (verified by TLC in 3:1 hexane/EtOAc). The reaction was quenched with 2 mL EtOAc and 2 mL water and further diluted with an additional 10 mL each EtOAc and water to facilitate separation. The separated aqueous layer was extracted with cold EtOAc (3 × 10 mL). The organic layers were combined and washed with saturated $NaHCO_3$, brine, and water (3 × 10 mL), dried over anhydrous $MgSO_4$, and filtered. Removal of the solvent *in vacuo* afforded product **3** as a light yellow gel containing a mixture of anomers (0.27 g, 0.82 mmol, 65 %).

$^1$H NMR (400 MHz $CDCl_3$): δ 5.56 (dd, 1H, H-3, *J* = 9.6, 10.4 Hz), 5.40 (d, 1H, H-1α, *J* = 3.2 Hz), 5.10 - 5.00 (m, 2H, H-4), 4.75 (d, 1H, H-1β, *J* = ), 4.32 - 4.22 (m, 3H), 4.17 - 4.10 (m, 2H), 3.92 (br s, 2H, OH), 3.75 - 3.71 (m, 1H), 3.51 (dd, 1H, H-2β), 3.44 (dd, 1H, H-2α, *J* = 3.22, 10.40 Hz), 2.09 (s, 3H), 2.09 (s, 2H), 2.08 (s, 3H), 2.08 (s, 2H) , 2.04 (s, 3H), 2.02 (s, 2H).

*Synthesis of 2-azido-2-deoxy-3,4,6-tri-*O*-acetyl-α,β-D-glucopyranosyl trichloroacetimidates (**4a** and **4b**).*

Synthesis with Sodium Hydride

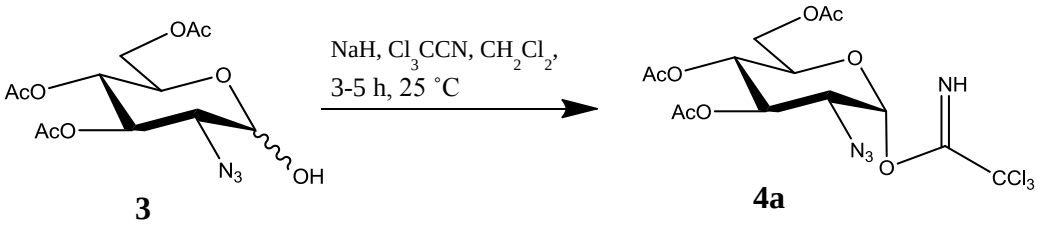


**3** **4a**

**Figure 2-4:** Synthesis of α-trichloroacetimidate **4a**.

0.20 g (0.60 mmol) **3** was dissolved in 5.8 mL dry $CH_2Cl_2$ in an oven dried round bottom flask. The solution was cooled to 0 °C in an ice water bath after which 47.0 mg (2 eq, 1.95 mmol) NaH (60 % dispersion in mineral oil) was added slowly with gentle stirring. A rubber septum and $N_2$ balloon were placed on the flask and 0.36 mL (6 eq, 3.59 mmol) $Cl_3CCN$ was added dropwise via syringe. The ice bath was removed and the mixture was allowed to stir at room temperature while monitoring by TLC in 2:1 hexanes: EtOAc for completion; about 3 – 5 hours. Upon completion the mixture was diluted with $CH_2Cl_2$, filtered through a celite pad, and concentrated *in vacuo*. The pure α-anomer (**4a**) was obtained by flash chromatography (2:1 hexane/EtOAc) to give 0.064g (0.13 mmol, 23 % yield).

$^1$H NMR (400 MHz $CDCl_3$): δ 8.83 (s, 1H, NHα), 6.50 (d, 1H, H-1, *J* = 3.60 Hz), 5.54 (dd, 1H, H-3, *J* = 9.40, 10.48 Hz), 5.17 (dd, 1H, H-4, *J* = 9.76 Hz), 4.30 (dd, 1H, H-6', *J* = 4.24, 12.36 Hz), 4.23 (ddd, 2H, H-5, *J* = 2.12, 4.14, 10.18 Hz), 4.11 (dd, 1H, H-6, *J* = 2.08, 10.24 Hz), 3.79 (dd, 2H, H-2, *J* = 3.6, 10.52 Hz ), 2.06 (s, 3H), 2.05 (s, 3H), 2.04 (s, 3H).

Synthesis with potassium carbonate

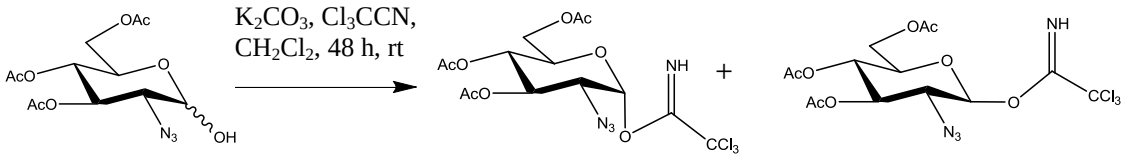


**3** **4a** **4b**

**Figure 2-5:** Synthesis of α/β-trichloroacetimidates **4a** and **4b**.

0.20 g (0.60 mmol) **3** was dissolved in 2.0 mL dry $CH_2Cl_2$. Anhydrous $K_2CO_3$ (0.21 g) was added slowly while stirring. 0.36 mL (3.59 mmol) $Cl_3CCN$ was added to the mixture dropwise via syringe. The reaction was stirred for 48 h under inert atmosphere then cooled to 0 °C, diluted with 0.60 mL $CH_2Cl_2$ and quenched by the addition of 0.50 mL $H_2O$. The layers were separated and the aqueous layer was extracted with $CH_2Cl_2$ (3 × 15 mL). The organic layers were combined and washed with brine (2× 15 mL), dried over $MgSO_4$, and concentrated under reduced pressure to give a brown sticky residue. The product was confirmed by NMR as a mixture of anomers (6:1; α:β). The successful purification of the α-anomer was not achieved during the time this procedure was used for the synthesis of **4**.

$^1$H NMR (400 MHz $CDCl_3$): δ 8.76 (s, 1H, NH-α), 8.73 (s, 1H, NH-β), 6.43 (d, 1H, H-1α, *J* = 3.6 Hz), 5.66 (d, 1H, H-1β, *J* = 8.4 Hz), 5.47 (dd, 2H, H-3, *J* = 9.2, 10.4 Hz), 5.10 (t, 1H, H-4, *J* = 10.0 Hz), 4.31 (dd, 1H, H-6', *J* = 4.24, 12.36 Hz), 4.23 (ddd, 2H, H-5, *J* = 2.12, 4.08, 10.2 Hz), 4.14 (dd, 1H, H-6, *J* = 2.08, 10.20 Hz), 3.72 (dd, 1H, H-2, *J* = 3.6, 10.52 Hz), 2.04 (s, 3H), 1.99 (s, 3H), 1.98 (s, 3H).

*Synthesis of (*S*)-2-hydroxy butan-1,4-dioic acid diallyl ester (**6**).*

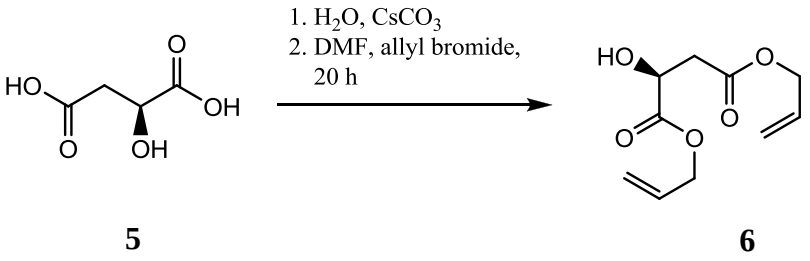


**5** **6**

**Figure 2-6:** Synthesis of diallyl malate **6**.

L-Malic acid **5** (2.5 g, 18.6 mmol) was dissolved in 5.0 mL D.I. water in a round bottom flask and neutralized to pH 7 by the addition of a concentrated solution of $Cs_2CO_3$. The reaction mixture was evaporated to dryness followed by azeotropic removal of residual water with MeOH (3 × 10 mL). The resulting white powder was resuspended in 15.0 mL anhydrous DMF, and a rubber septum and $N_2$ balloon were placed on the flask. Allyl bromide (5.4 mL, 0.062 mol) was added dropwise. The reaction mixture was stirred for at least 20 h after which it was quenched by pouring over 125 mL crushed ice. The separated aqueous layer was extracted with EtOAc (3 × 25 mL). The combined organic layers were washed with saturated $NaHCO_3$ (25 mL), water (3 × 10 mL), and brine (20 mL), dried over $MgSO_4$, and concentrated *in vacuo*. The pure product **6** was obtained by flash chromatography (2:1; hexanes/EtOAc) as a yellow oil (1.19 g, 5.6 mmol, 30 %).

$^1$H NMR (400 MHz $CDCl_3$): δ 5.98 - 5.85 (m, 2H), 5.36 - 5.23 (m, 2H), 4.70 (dt, 2H, *J* = 1.28, 5.84 Hz), 4.62 (dd, 2H, *J* = 1.34, 5.76 Hz), 4.55 (dd, 1H, *J* = 1.06, 5.74 Hz), 3.18 (d, 1H, *J* = 5.48 Hz), 2.93 (dd, 1H, *J* = 4.48, 16.04 Hz), 2.86 (dd, 1H, *J* = 6.04, 16.04 Hz).

*Glycosylation*

Synthesis of 2-(*S*)-(3,4,6-tri-*O*-acetyl-2-azido-2-deoxy-α-D-glucopyranosyl)-butan-1,4-dioic acid diallyl ester (**7**).

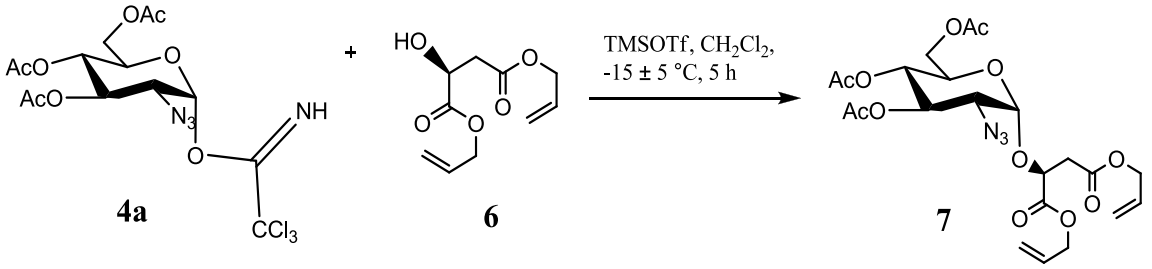


**Figure 2-7:** Synthesis of diallyl malate ester **7**.

In an oven dried reaction flask 0.110 g (0.23 mmol) **4a** was dissolved in 4.8 mL dry $CH_2Cl_2$. A small amount of 4 Å molecular sieves and 0.059 g (0.28 mmol) **6** were then added. The reaction was cooled to approximately -35 °C before 0.20 mL TMSOTf was added via syringe. The mixture was stirred for 5 hours while the temperature was maintained at -15 ± 5 °C. The reaction was quenched with 1.5 mL of a saturated $NaHCO_3$ solution, and 1.0 mL $H_2O$. The layers were separated and the aqueous layer was extracted with $CH_2Cl_2$ (2 × 15 mL). The organic layers were combined, washed with brine, dried over $MgSO_4$, and concentrated *in vacuo*. The product was purified by flash chromatography using a 2:1 solution of hexanes: ether to elute excess **6** followed by elution of the product with ether. The pure α-anomer (**7**) was recovered as a light brown syrup (0.071 g, 0.15 mmol, 67 %).

$^1$H NMR (400 MHz $CDCl_3$): δ 5.84-5.80 (m, 2H), 5.45 (dd, 1H, H-3, *J* = 9.28, 10.76 Hz), 5.32-5.14 (m, 4H), 5.12 (d, 1H, H-1, *J* = 3.8), 5.03 (dd, 1H, H-4, *J* = 9.28, 10.36 Hz), 4.64 - 4.62 (m, 5H), 4.45 (dt, 1-H, H-5, *J* = 3.0, 10.4 Hz), 4.22 (dd, 1H, H-6', *J* =

3.56, 12.60 Hz), 3.91 (dd, 1H, H-6, *J* = 2.20, 12.6 Hz), 3.24 (dd, 1H, H-2, *J* = 3.76, 10.76 Hz), 2.00 (s, 3H), 1.99 (s, 3H), 1.96 (s, 3H).

Synthesis of 2-(*S*)-(3,4,6-tri-*O*-acetyl 2-azido-2-deoxy-α-D-glucopyranosyl)-hydroxysuccinate ester (**9**).

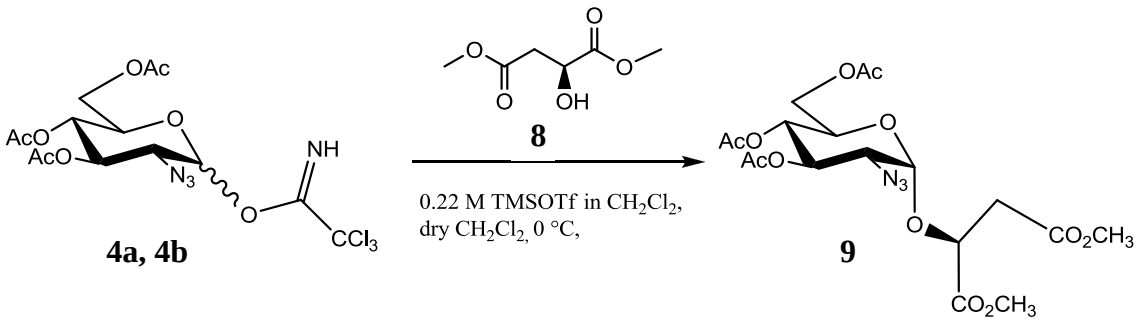


**Figure 2-8:** Synthesis of dimethyl malate ester **9**.

0.05 mL (0.06 g, 0.38 mmol) dimethyl-(*S*)-malate was added to a solution of **4a** and **4b** (0.15 g, 0.32 mmol) in 0.5 mL dry $CH_2Cl_2$. After allowing the mixture to stir 30 minutes at room temperature under inert atmosphere, the solution was cooled to 0 °C. A 0.22 M solution of TMSOTf in $CH_2Cl_2$ (0.15 mL, 3.30 μmol) was then added dropwise while continuing to stir on ice. The reaction was quenched after 1 hour 20 minutes with 1.0 mL $Et_3N$, and filtered through celite. The crude product contained a mixture of dimethyl malate ester **9**, excess unreacted **8**, and glucopyranoside **3**; as verified by $^1H$ NMR. Product **9** was never successfully purified from the reaction mixture.

*Synthesis of* N-*(tert-butoxycarbonyl)*-S-*trityl*-*L*-*cysteine pentafluorophenyl ester (**11**).*

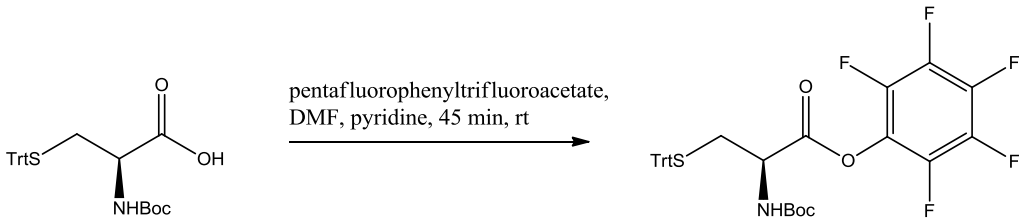


**10** **11**

**Figure 2-9:** Synthesis of cysteine pentafluorophenyl ester **11**.

*N*-Boc-Cys(TrtS)-OH (**10**) (0.557 g, 1.2 mmol) was dissolved in anhydrous DMF (2.2 mL) and pyridine (0.2 mL). Pentafluorophenyltrifluoroacetate (0.37 mL, 2.2 mmol) was added dropwise and the reaction mixture was stirred for 45 minutes at room temperature, monitoring for completeness by TLC in 9:1, $CHCl_3$/hexane. Upon completion the reaction mixture was diluted with additional $CHCl_3$ (25 mL), washed with water (3 × 15 mL), and dried over $Na_2SO_4$. The solvent was removed *in vacuo* and the purified product was obtained after flash chromatography (9:1; $CHCl_3$/EtOAc) to give product **11** as a pale yellow wax (0.86 g, 1.36 mmol, 61 % yield).

$^1$H NMR (400 MHz $CDCl_3$): δ 7.44 - 7.42 (m, 6H), 7.32 - 7.28 (m, 6H), 7.24 - 7.21 (m, 3H), 4.99 (d, 1H, *J* = 7.2 Hz), 4.33 (d, 1H, *J* = 6.68, 11.8 Hz), 2.84 (dd, 1H, *J* = 6.4, 12.4 Hz), 2.69 (dd, 1H, *J* = 4.80, 12.80 Hz), 1.44 (s, 9H).

*Attempted synthesis of 2-(*S*)-(3,4,6-tri-*O*-acetyl-2-[*N*-(tert-butoxycarbonyl)-*S*-trityl-L-cysteinyl)amino]-2-deoxy-α-D-glucopyranosyl)-butan-1,4-dioic acid diallyl ester (**12**).*

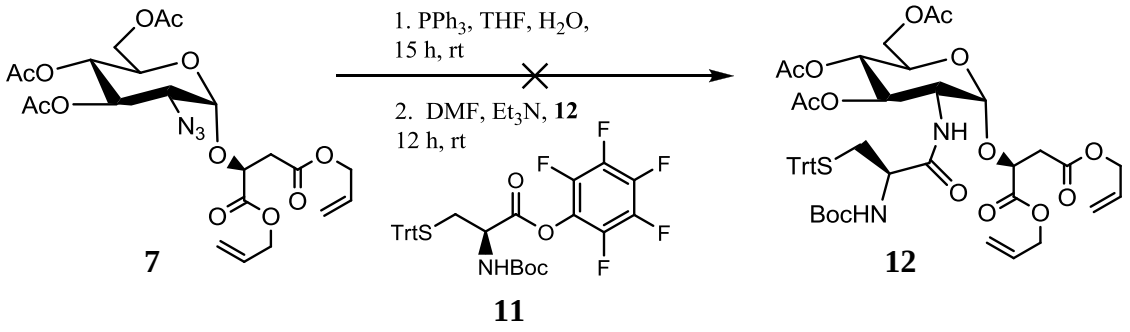


**Figure 2-10:** Attempted synthesis of cysteinyl diallyl malate ester **12**.

0.030 g (58.3 µmol) of glycoside **7** was dissolved in THF (1.2 mL) and $H_2O$ (0.3 mL). Triphenylphosphine (0.052 g) was then added to the solution and the reaction was allowed to stir 15 hours. The solvent was then removed under reduced pressure and the residual $H_2O$ was removed azeotropically with toluene. The sticky residue that resulted was triturated with hexanes to remove excess triphenylphosphine oxide. DMF (0.37 mL) was then added to the reaction flask to dissolve the residue and **11 (**0.043 g, 68.2 µmol) was added followed by the addition of 0.02 mL $Et_3N$. The reaction was allowed to stir under inert atmosphere for 12 hours after which the solution was diluted with EtOAc (3 mL). The organic layers were washed with saturated $NaHCO_3$ (10 mL), $H_2O$ (10 mL), and brine (10 mL). After drying over anhydrous $MgSO_4$ the product was filtered and concentrated under reduced pressure. The crude mixture was found to contain triphenylphosphine oxide and unreacted starting materials by $^1H$ NMR.

*Determination of minimum inhibitory concentration (MIC) of fosfomycin in* B. subtilis.

3.0 mL of sterile nutrient media was inoculated with *B. subtilis* cells from glycerol stock. The culture was incubated overnight at 37 °C with shaking at 150 rpm. 200 µL of overnight culture was then plated onto a nutrient media/agar culture plate. Paper discs were applied to the plate and 5.0 µL of fosfomycin solutions of varying concentrations were pipetted onto the paper discs. Sterile $H_2O$ was also added to a paper disc as a control. The plate was incubated overnight at 37 °C. Growth inhibition was observed as halos around the paper discs in which no cell growth could be seen. The diameters of the halos were measured in mm.

# Chapter 3: Results and Discussion

The metabolism of BSH has been identified as a potential target for drug therapy, yet its functions have not been fully elucidated. Considering that it has been difficult to obtain sufficient quantities of BSH from cell cultures for biological testing (*26*), a chemical approach was taken toward its synthesis. At the start of this study there were no published methods for the synthesis of BSH. A synthetic scheme was proposed based on known procedures for the synthesis of *O*-glycosides. BSH is an α-anomeric glycoside of L-cysteinyl-D-glucosamine with L-malic acid (*21*). Its synthesis, therefore, requires the formation of an α-glycosidic bond at C-1 of D-glucosamine with L-malic acid and a peptide bond at C-2 with L-cysteine. For this reason the trichloroacetimidate method described by Rele and colleagues was employed for the synthesis of a suitable glycosyl donor (*32*). D-glucosamine · HCl, (**1)** which is commercially available, was used as the precursor for the synthesis of the trichloroacetimidate donor (**4**).

The first step in the synthesis of **4** was to introduce the non-participating azide group at C-2 of glucosamine (**1**) using triflic azide ($TfN_3$). $TfN_3$ is not available commercially and so it was necessary to prepare it by treating $NaN_3$ with $Tf_2O$. Since $TfN_3$ is explosive it was kept in a solution of $CH_2Cl_2$ and was either used immediately or stored temporarily at -20 ºC. Infrared spectroscopy was used to verify the azide linkage to the triflate by the presence of a sharp peak at around 2100 $cm^{-1}$ (2153 cm $^{-}$1) that is characteristic for bound azides (Fig. 3-1).

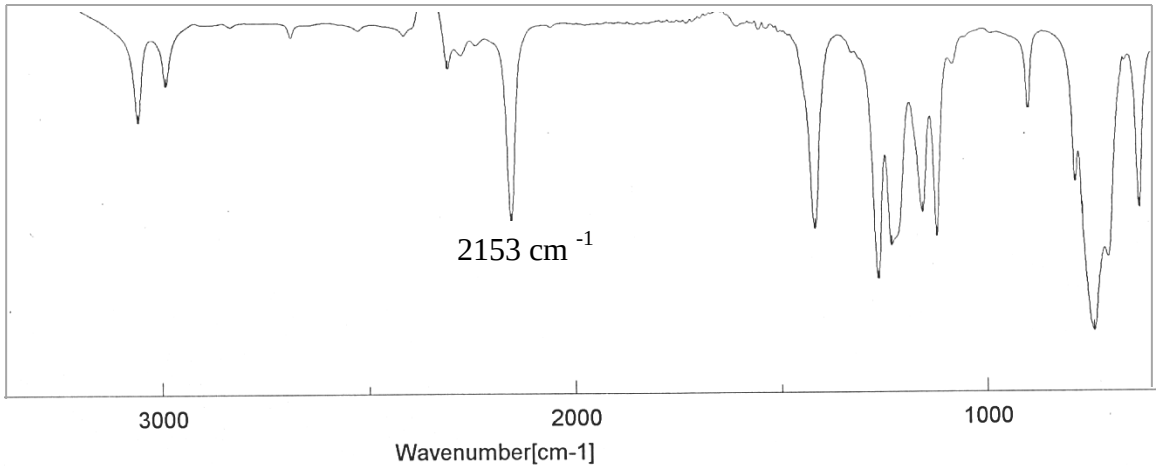


**Figure 3-1**: Infrared spectrum of triflic azide in $CH_2Cl_2$.

This solution of $TfN_3$ was then cannulated under positive pressure of $N_2$ into a reaction flask containing glucosamine (**1**) and DMAP in methanol in order to maintain an inert atmosphere. Acetate protecting groups were then introduced through acetylation with anhydrous acetonitrile and pyridine. Purification by flash column chromatography (3:1, hexanes/EtOAc) afforded acetate **2** (59 % yield). $^1$H NMR spectroscopy was used to verify the presence of the acetate groups as two 6H singlets, and four 3H singlets that appear at 2.21 - 2.04 ppm (Fig. 3-2). The successful linkage of the azide group was confirmed by the sharp peak observed at 2153 cm$^{-1}$ in the IR spectrum (Fig. 3-3).

.

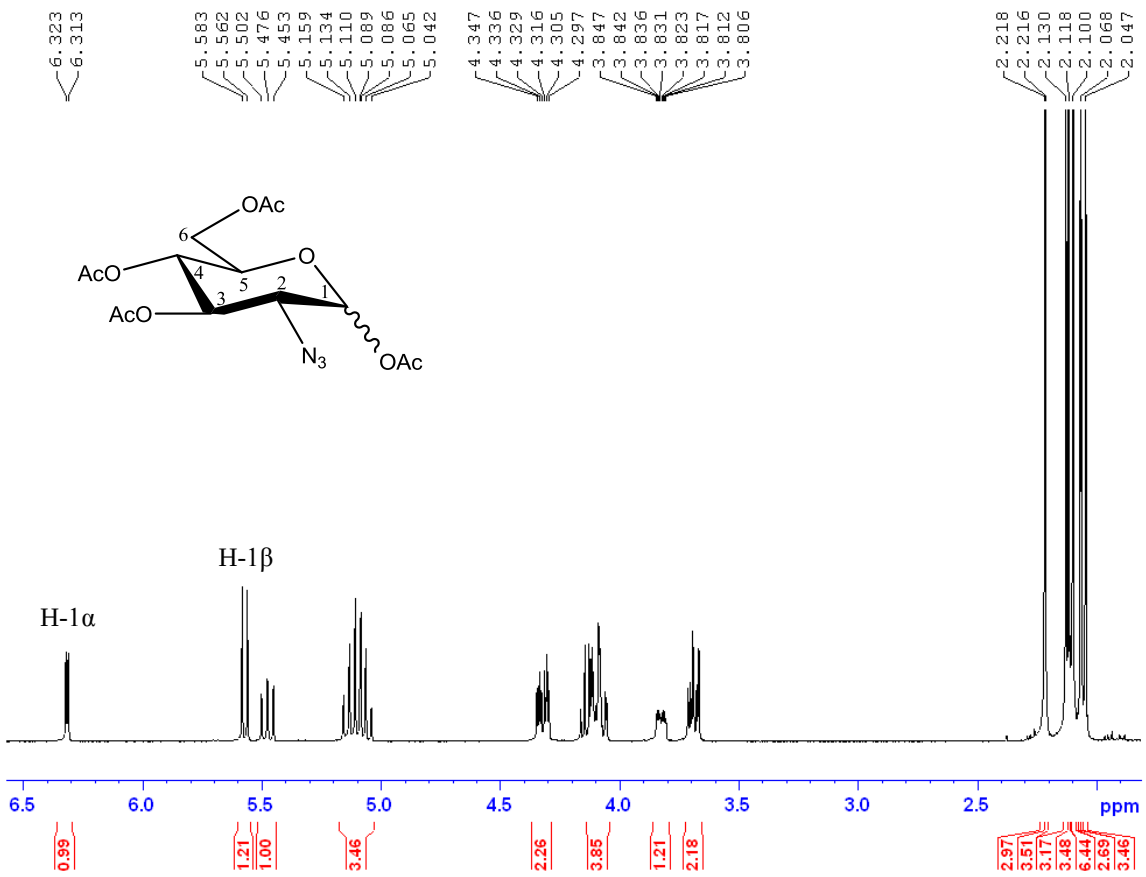


**Figure 3-2**: 400 MHz $^{1}$H NMR of glucopyranosyl acetate **2** in $CDCl_3$.

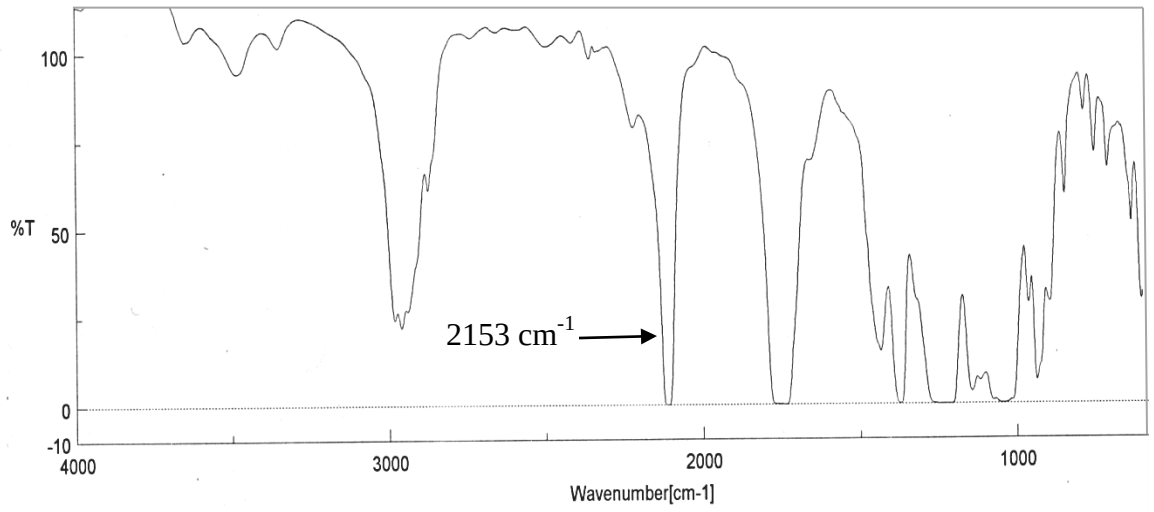


**Figure 3-3**: Infrared spectrum of acetate **2**.

The selective hydrolysis of the anomeric acetate was achieved by the addition of hydrazine acetate and DMF to give glucopyranoside **3** (65 % yield). Evaluation of **3** by $^{1}$H NMR confirmed the presence of the hydroxyl proton as a broad singlet at 3.92 ppm as seen in figure 3-4. A downfield shift of the anomeric protons also verified that the electron-withdrawing acetate group was replaced by a hydroxyl group. IR spectroscopy was also used to verify that the azide group was still present (Fig. 3-5). This was confirmed by the sharp peak at 2153 $cm^{-1}$. Presence of the hydroxyl group could also been seen in the IR spectrum as a broad OH stretch around 3455 $cm^{-1}$. Deviating from the literature procedure, glucopyranoside **3** was used without purification by column chromatography. Rather, the product was washed with additional portions of $H_2O$ after the aqueous workup to remove the excess DMF, as it was the only notable impurity seen in the NMR spectrum (seen as two singlets at 2.96 ppm and 2.88 ppm). However, small amounts of residual DMF do not seem to affect the conversion of **3** to trichloroacetimidates **4a** and **4b**.

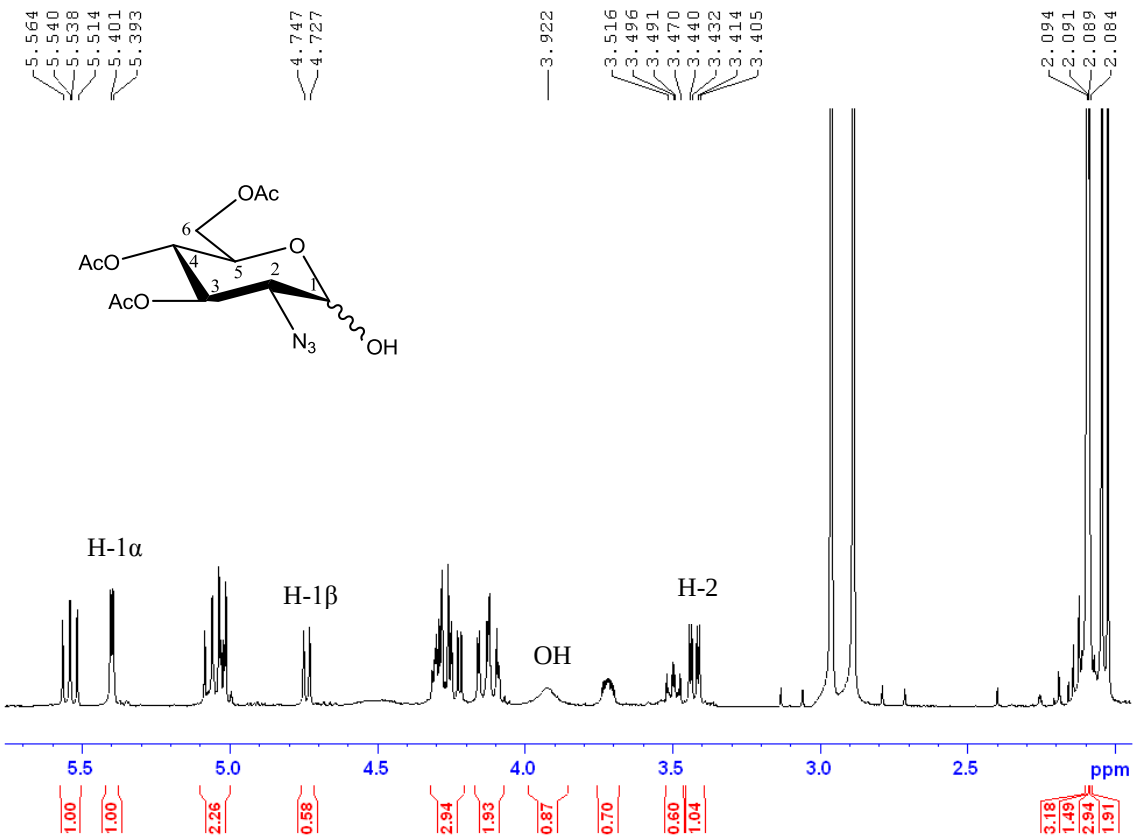


**Figure 3-4:** 400 MHz $^{1}$H NMR of glucopyranoside **3** in $CDCl_3$.

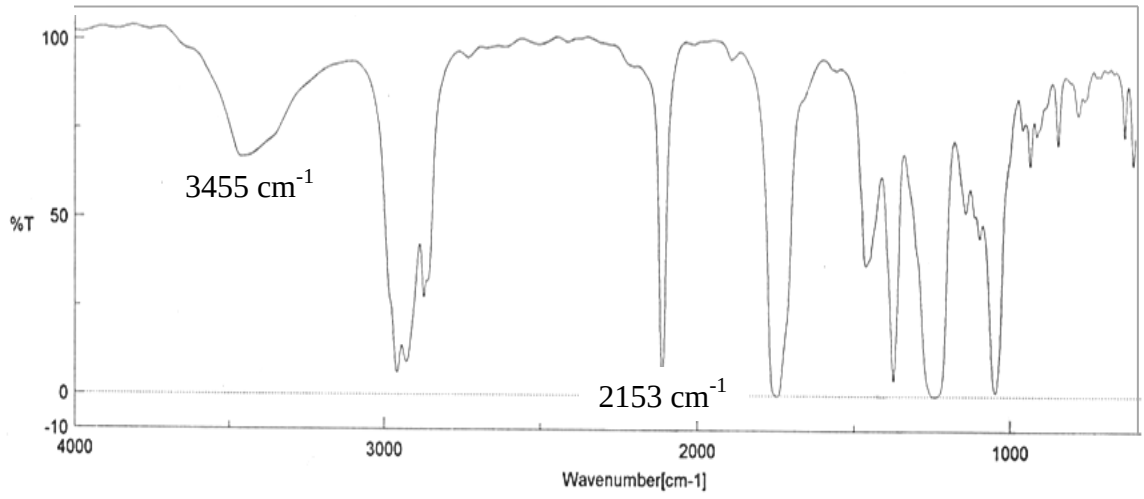


**Figure 3-5:** Infrared spectrum of glucopyranoside **3**.

Glucopyranoside **3** was treated with trichloroacetonitrile in the presence of anhydrous potassium carbonate to give an anomeric mix of trichloroacetimidates **4a** and **4b**. NMR spectroscopy was used to confirm the linkage of the imidate (Fig. 3-6). Singlets observed at 8.76 ppm and 8.73 ppm indicate the imidate protons of the α and β anomers respectively. A downfield shift was also seen for the H-1α and H-1β protons, from 5.40 ppm and 4.74 ppm respectively, to 6.43 ppm and 5.66 ppm respectively due to the replacement of the hydroxyl group with the electron-withdrawing imidate group. This also caused the H-2 proton to experience a downfield shift from 3.44 ppm to 3.72 ppm. The sharp peak at 2153 $cm^{-1}$ in the IR spectrum verified that the azide moiety at C-2 was conserved (Fig. 3-7).

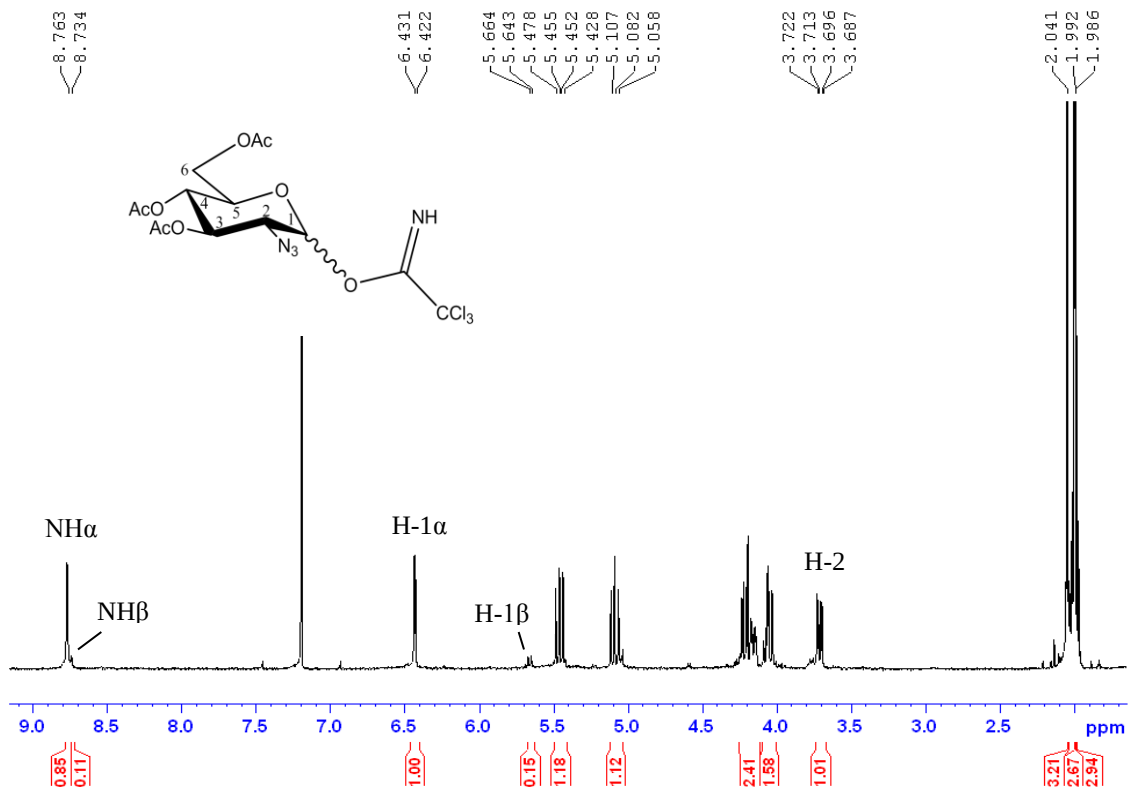


**Figure 3-6:** 400 MHz NMR of trichloroacetimidates **4a** and **4b** in $CDCl_3$.

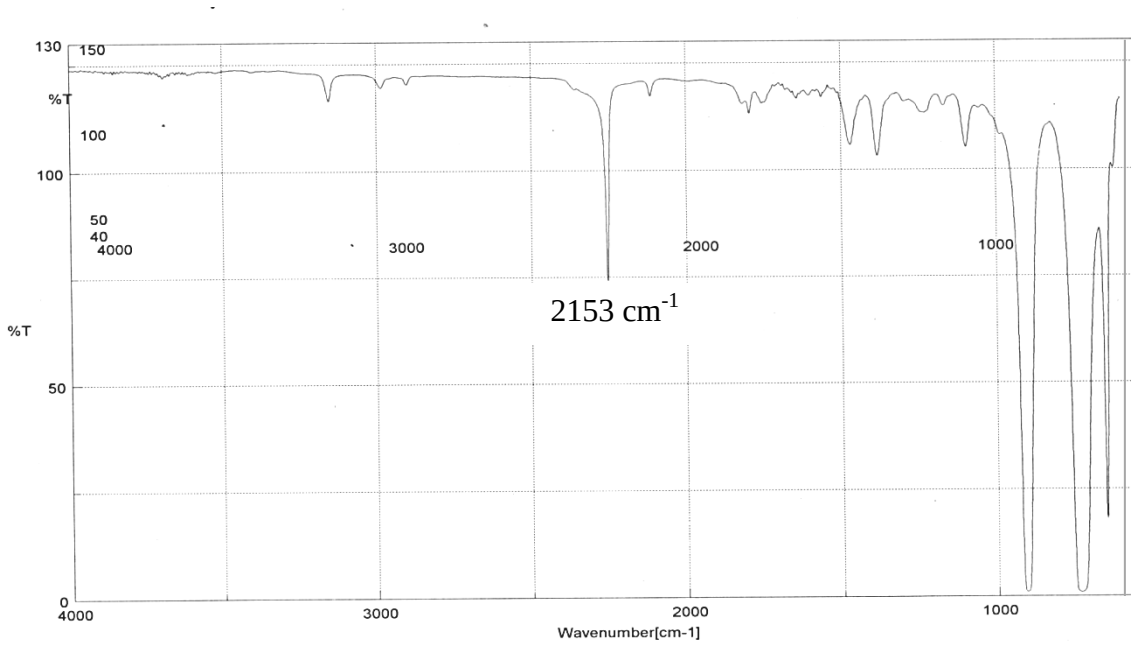


**Figure 3-7:** Infrared spectrum of trichloroacetimidates **4a** and **4b**.

Trichloroaceimidate **4** was stored at -20 °C as a solution in $CH_2Cl_2$ as it is unstable at room temperature. Several attempts to purify **4a** were unsuccessful. For this reason efforts were made to form the glycoside from the mixture of **4a** and **4b** (**4**) with malate **8**. This was done using the literature procedure described by Rele (*32*) for the glycosidic linkage of **4** with 4-penten-ol; replacing 4-penten-ol with dimethyl malate **8**. A solution of **4** and **8** was treated with a 0.22 M solution of TMSOTf in $CH_2Cl_2$ at 0 °C to give glucopyranosyl dimethyl malate ester (**9**). $^1$H NMR analysis of the crude product showed that product **9** was present as well as unreacted **8** (Fig. 3-8). The disappearance of the imidate proton signals at 8.76 ppm and 8.73 ppm and the upfield shift of H-1α and H-1β to 5.39 ppm and 4.74 ppm respectively verified that the imidate group was hydrolyzed. Some of the hydrolyzed donor was left unreacted and could be seen as glucopyranoside **3** in the spectrum. An upfield shift was seen for H-1α from 6.49 ppm to 5.18 ppm as well as for the H-2 signal, from 3.72 ppm to 3.30 ppm, indicating the successful linkage of **8**. COSY NMR was then used to confirm the correlation between H-1 and H-2 in compound **9**. The relationship between H-1α and H-1β with H-2 of compound **3** was also verified by the COSY spectrum. Although the synthesis of **6** was successful, attempts to purify the product from the crude reaction mixture failed. TLC analysis of the crude reaction mixture showed that product **9** and unreacted **8** have similar $R_f$ values in a variety of solvent systems, making them difficult to separate by flash chromatography.

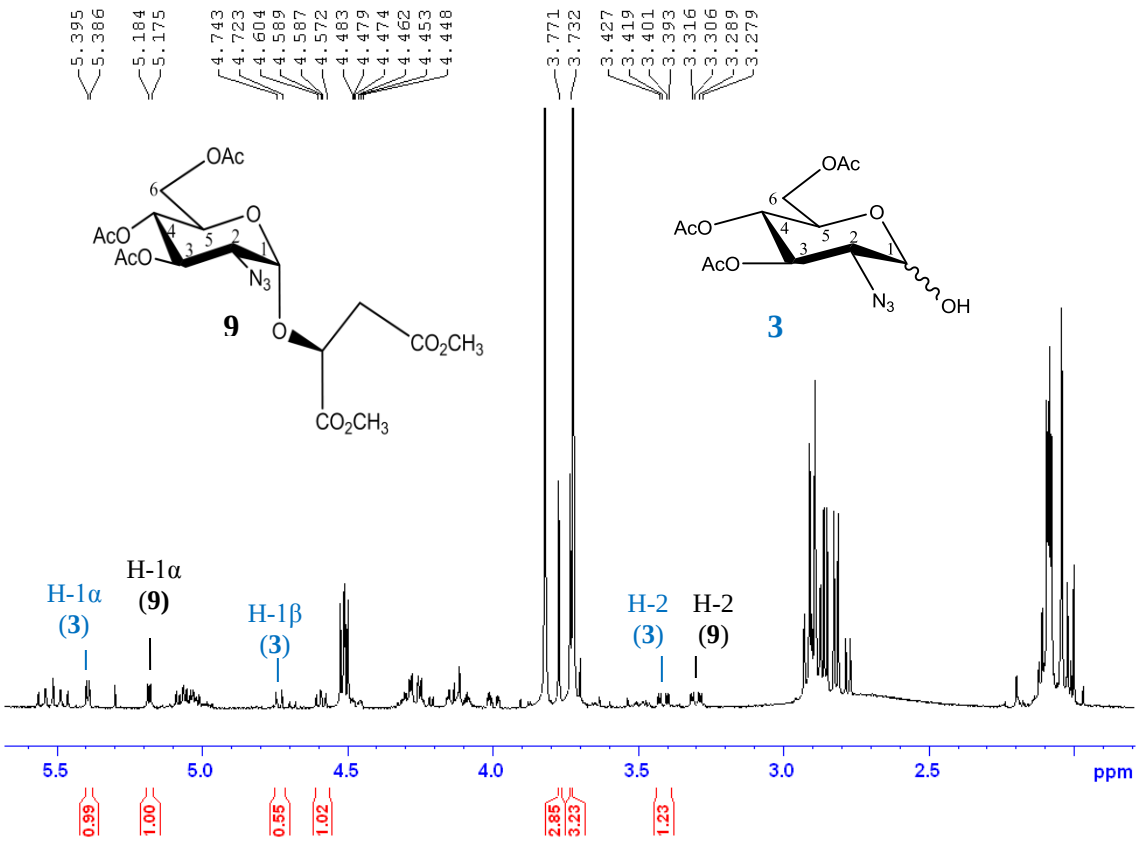


**Figure 3-8:** 400 MHz $^{1}$H NMR of dimethyl malate ester **9** crude reaction mixture in $CDCl_3$.

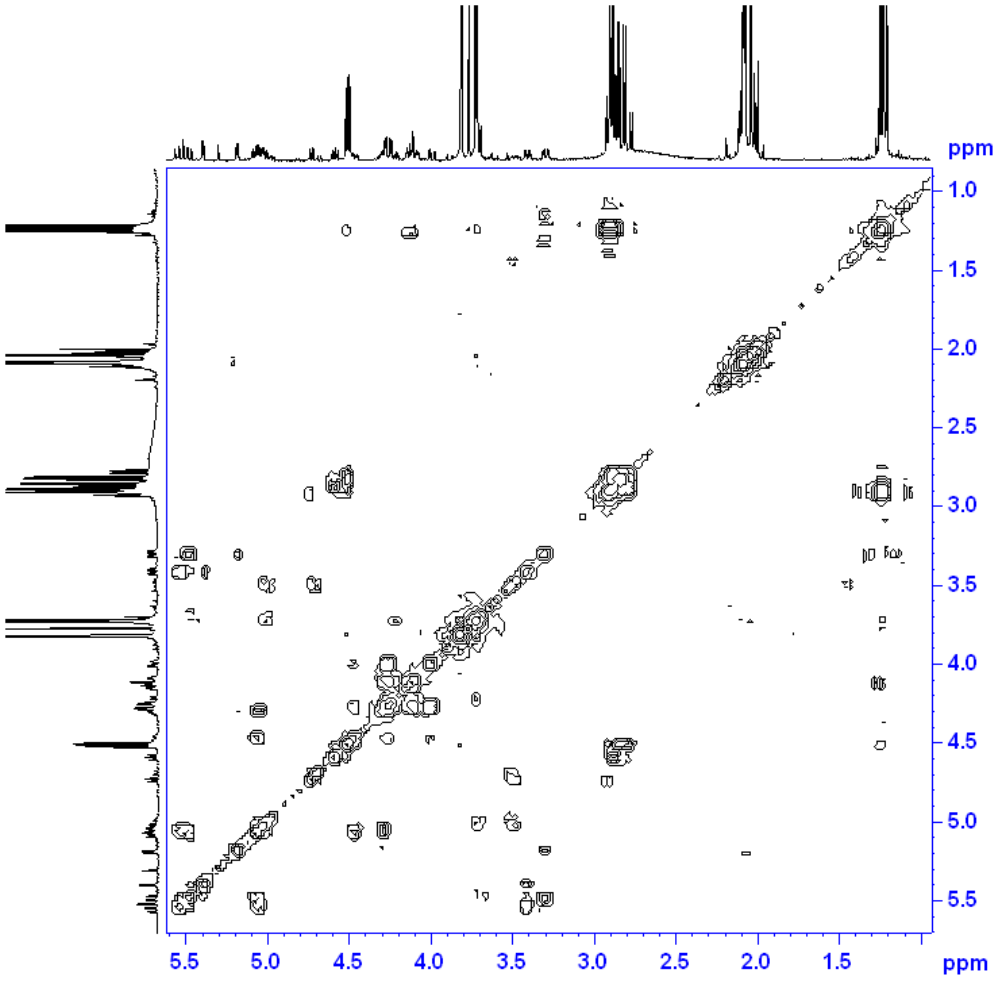


**Figure 3-9:** 400 MHz COSY NMR spectrum of dimethyl malate ester **9** crude reaction mixture in $CDCl_3$.

At this time it was discovered that a method for the synthesis of BSH had very recently been published by Sharma *et al* (*25*). The trichloroacetimidate method was also employed by Sharma and colleagues for the formation of the *O*-glycoside, however, using only the α-anomer. They also investigated several methods of protection for the malate aglycone including benzyl, methyl and allyl groups. Although they were successful in synthesizing glycosides from **4a** with all three of these malate esters, deprotection of the benzyl- and dimethyl-malate esters proved problematic. A variety of

deprotection strategies were investigated; however, all efforts resulted in cleavage of the aglycone or decomposition. Successful deprotection was only reported when the allyl protecting groups were used. For this reason, the synthesis of ester **9** was not pursued any further and attention was turned toward the synthesis of ester **7**.

Since the work by Sharma and colleagues (*25*) described the use of only the pure α-trichloroacetimidate, purification of the crude mixture was reinvestigated, as well as a faster method for the synthesis of **4**. In the procedure described by Rele (*32*), $K_2CO_3$ was used as the base catalyst in the presence of $CCl_3CN$ and the reaction took 48 hours to complete. It was found that the use of NaH as the base gave the desired product in only 3-5 hours. Both methods were found to give a mix of α and β anomers in about a 6:1 ratio respectively. It should be noted that it is necessary to add the NaH slowly to avoid the generation of heat and the consequential decomposition of the carbohydrate ring. Purification of **4a** was eventually achieved by flash chromatography using 2:1 hexanes/EtOAc and was confirmed by NMR shown in figure 3-10.

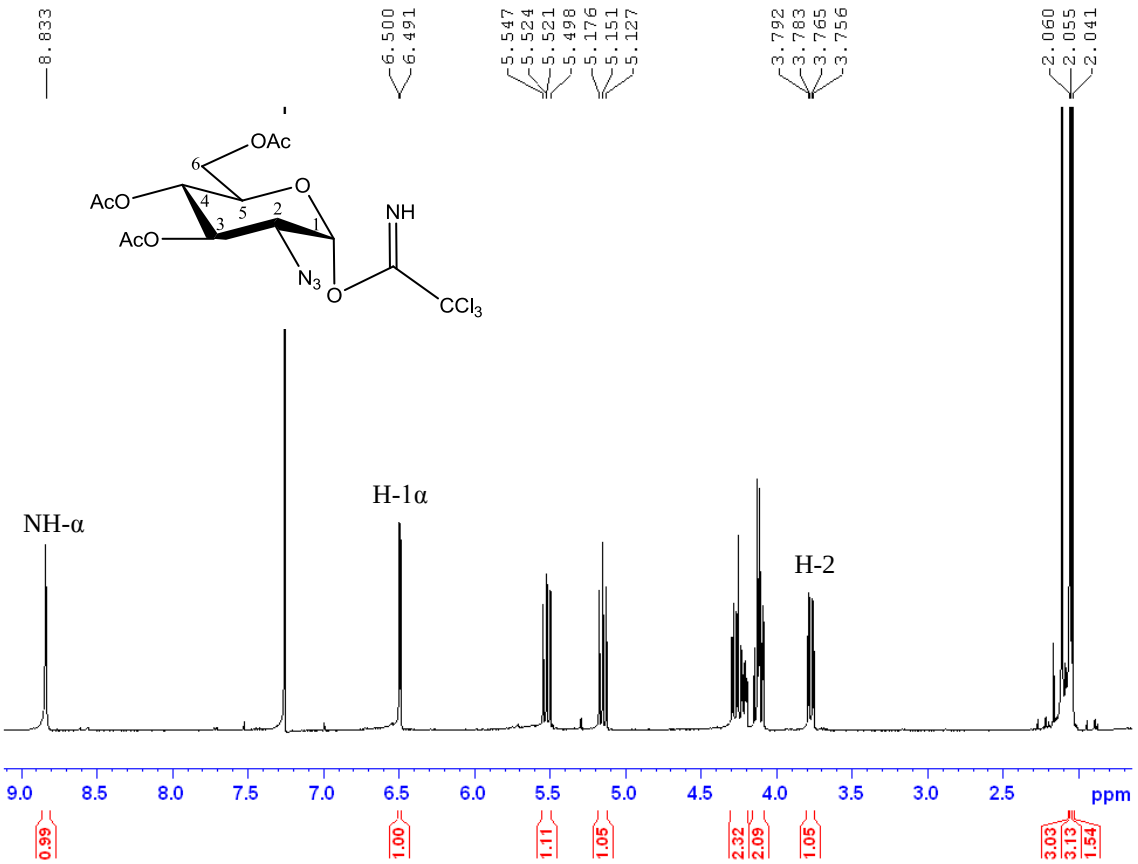


**Figure 3-10:** 400 MHz $^{1}$H NMR of α-trichloroacetimidate (**4a**) in $CDCl_3$.

Malate **6** is not commercially available; therefore, it was synthesized from L-malate (**5**) and allyl bromide. An aqueous solution of **5** was neutralized to pH 7 using a 6.5 M solution of $Cs_2CO_3$ and evaporated to dryness under reduced pressure. Any residual water was azeotropically removed with portions of methanol. The resulting white powder was redissolved in anhydrous DMF and treated with allyl bromide. Pure **6** was obtained after flash chromatography (2:1; hexanes/EtOAc). $^{1}$H NMR were used to confirm the synthesis of **6** (Fig. 3-11). The apperarnce of a 2H multiplet from 5.91 - 5.75 ppm and a 4H multiplet in the range of 5.29 - 5.15 ppm indicated the presence of the allylic protons. The attachment of the allyl protecting groups was also confirmed by the disappearance of the 3H singlet at 4.79 ppm and the appearance of a 1H doublet at 3.18

ppm. This indicates that the carboxylic OH protons are no longer present and one OH signal remains.

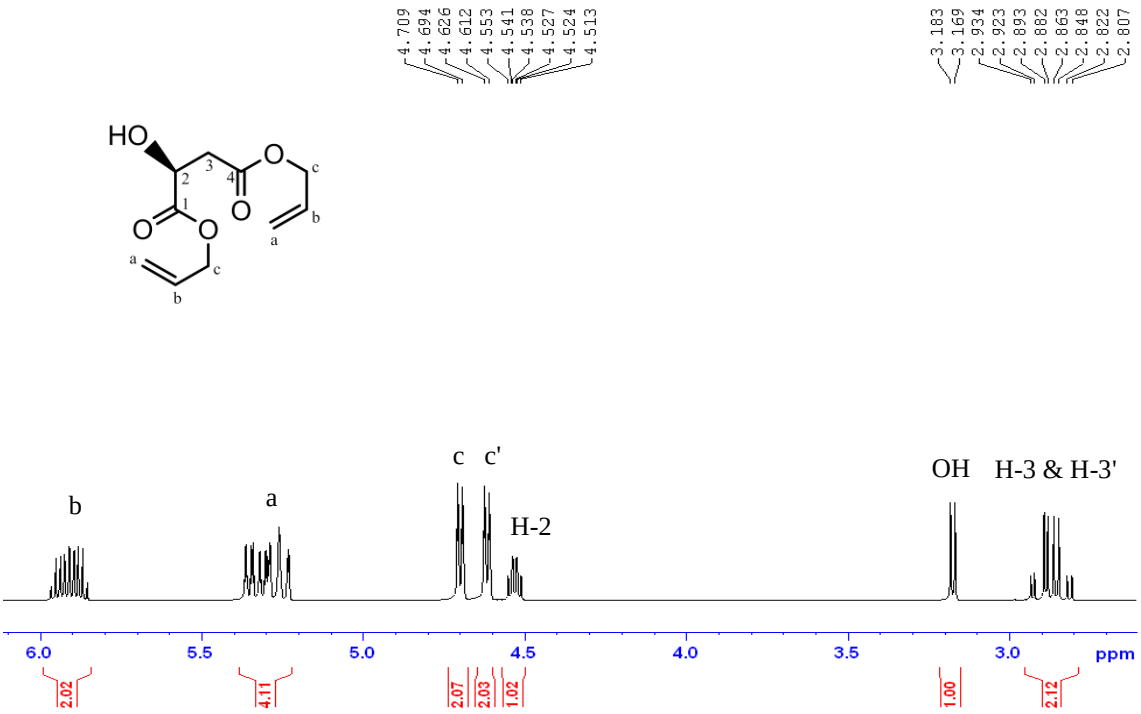


**Figure 3-11**: 400 MHz $^{1}$H NMR of diallyl malate **6** in $CDCl_3$.

The synthesis of compound **7** was accomplished by reacting malate **6** with **4a** in dry $CH_2Cl_2$ in the presence of TMSOTf as described by Sharma *et al* (*25*). This reaction requires dry conditions, therefore, the reaction was carried out in an oven dried flask and molecular sieves were added to the reaction mixture; dry solvents were also used. The reaction conditions call for the reaction mixture to be cooled to -35 ºC and then maintained at -15 ± 5 ºC for 5 hours. This was done by using mixtures of ethylene glycol and ethanol with dry ice as described by Jensen and Lee (*34*). The use of excess diallyl malate is required for the reaction to proceed. However, it was found that a 1:1.1 molar ratio of **4a**: **6** is adequate rather than the 1:1.48 molar ratio described in the literature.

This ratio resulted in less unreacted malate in the crude product. Compound **7** was purified from the crude mixture by column chromatography. A 2:1 hexanes: ether solvent system was first used to elute excess **6**. The product (**7**) was then eluted from the column with pure ether. $^{1}$H and COSY NMR were used to confirm the synthesis of **7** (Fig. 3-12 and Fig. 3-13 respectively). The upfield shifts of the H-1α doublet from 6.50 ppm to 5.13 ppm and the H-2 doublet of doublets from 3.79 ppm to 3.24 ppm indicates that the imidate group was replaced by the less electron-withdrawing malate moiety. The disappearance of the OH singlet at 3.18 ppm seen in compound **6** confirmed its linkage to **4a**. COSY NMR was used to verify the correlation between H-1α and H-2.

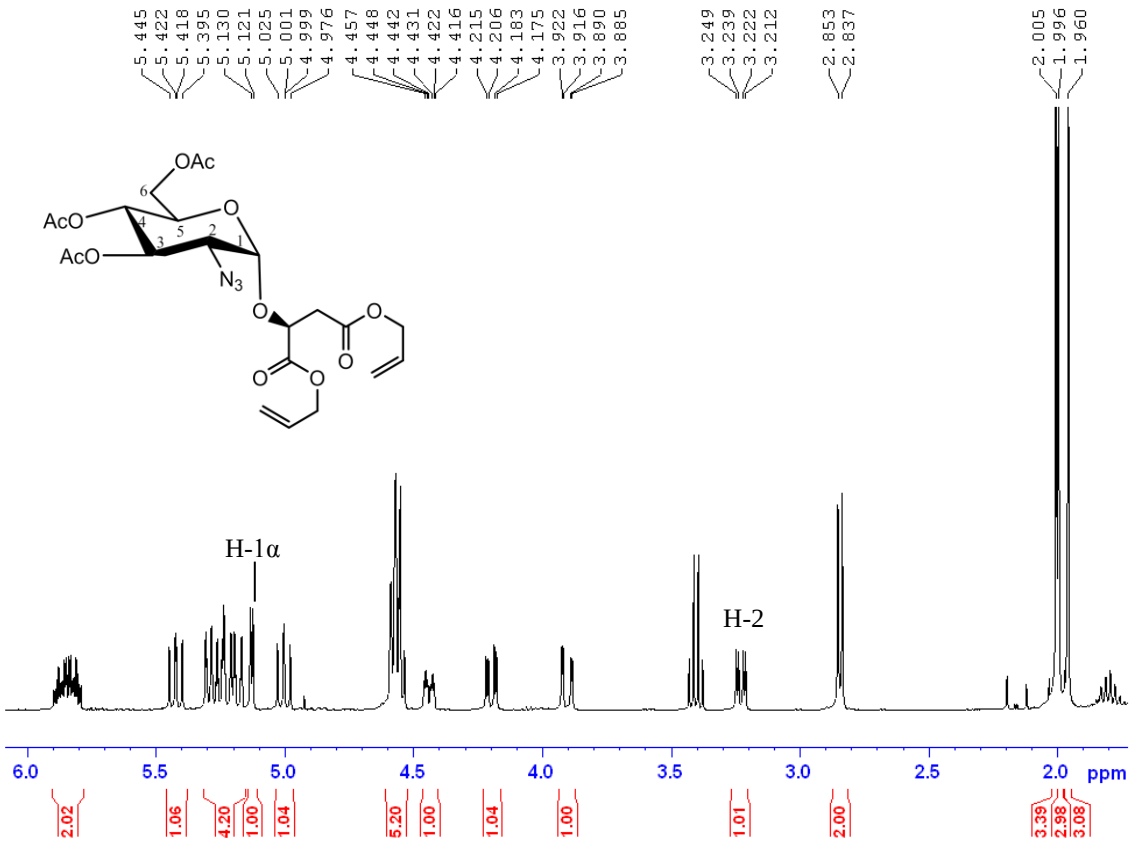


**Figure 3-12:** 400 MHz $^{1}$H NMR of diallyl malate ester **7** in $CDCl_3$.

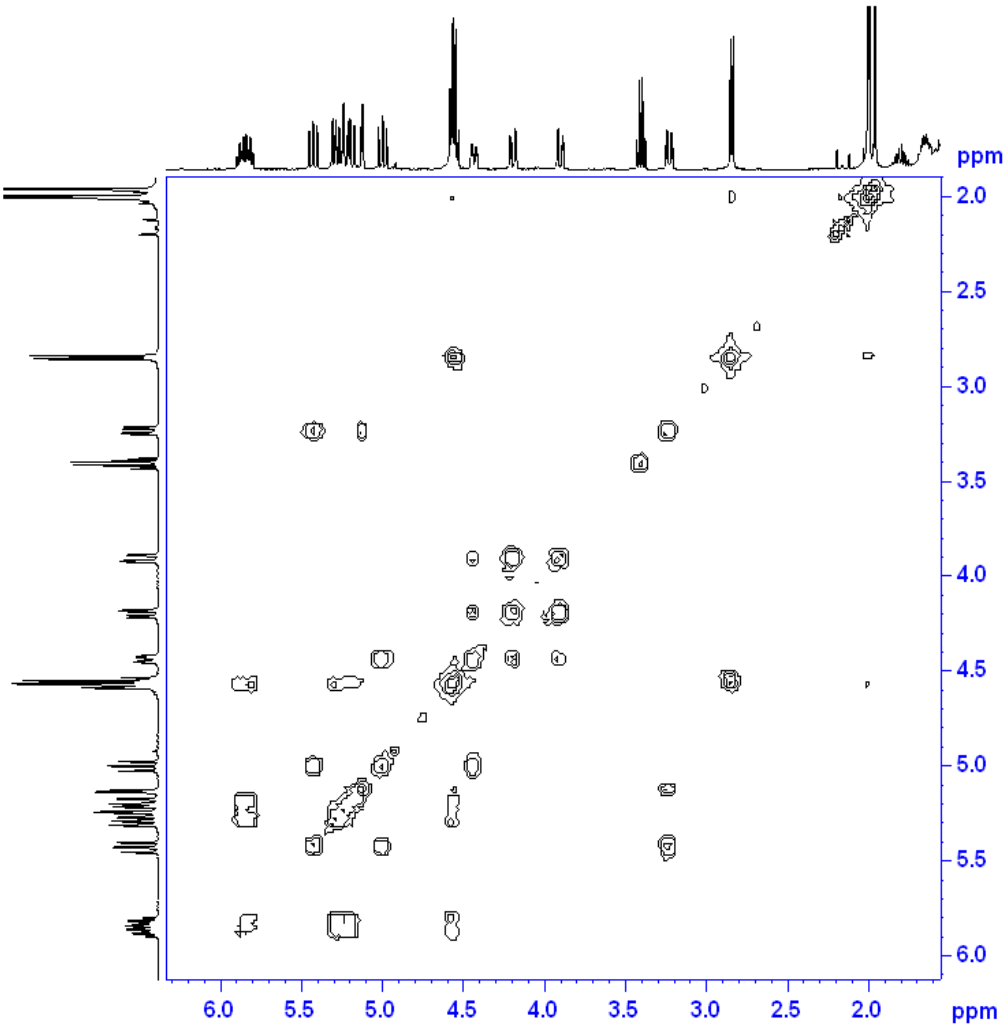


**Figure 3-13:** 400 MHz COSY of diallyl malate ester **7** in $CDCl_3$.

The method described by Sharma *et al* (*25*) for the introduction of the peptide bond at C-2 involves a Staudinger reduction of the azide to an amine using triphenylphosphine and the subsequent ligation of cysteine **11** in the presence of HOBt and $Et_3N$. Due to the explosive nature of HOBt an attempt was made to introduce the peptide bond using only **11** as the activated ester in the presence of a base (*33*). Since **11** is not commercially available it was synthesized from *N*-Boc-Cys(Trt)-OH (**10**) through treatment with pentafluorophenyltrifluoroacetate in a solution of DMF and pyridine. The

linkage of the activating group was confirmed by $^{1}$H NMR (Fig. 3-14) as the disappearance of the OH singlet at 2.65 ppm and the appearance of two 1H doublet of doublets at 2.84 ppm and 2.69 ppm ( $J$ = 6.4, 12.4 Hz $J$ = 4.80, 12.80 Hz respectively). The presence of the 9H singlet at 1.44 ppm indicates that the *tert*-butoxycarbonyl protecting group remained intact.

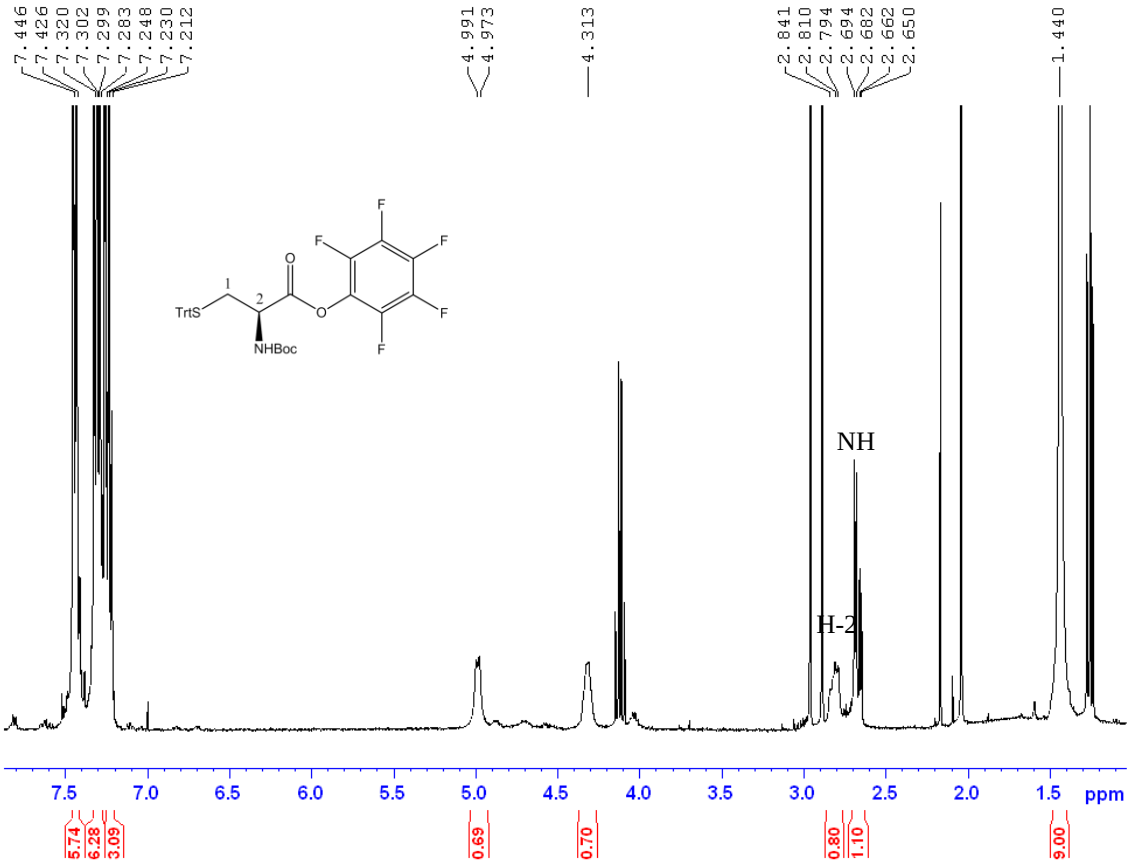


**Figure 3-14:** 400 MHz $^{1}$H NMR of cysteine pentafluorophenyl ester **11** in $CDCl_3$.

An attempt was made to link cysteine **11** at C-2 of ester **7** by first reducing the azide at C-2 to an amine. This was done by treating ester **7** with $PPh_3$ in THF and $H_2O$, followed by the removal of $Ph_3PO$ by trituration with hexanes. IR spectroscopy was used to confirm the reduction of the azide to the free amine by the disappearance of the

characteristic azide peak at 2153 $cm^{-1}$ (Fig. 3-15). A peak at around 2955 $cm^{-1}$ in the IR spectrum indicated that $Ph_3PO$ remained in the reaction mixture. Further efforts to remove the residual $Ph_3PO$ by trituration with hexanes were unsuccessful. The addition of **11** and $Et_3N$ in a solution of DMF was carried out in an attempt to couple compound **11** with the reduced compound **7**. However, $^1H$ NMR of the crude mixture showed that the diallyl malate aglycone was hydrolyzed and the carbohydrate was decomposed. Significant amounts of $Ph_3PO$ and **11** were also seen in the NMR spectrum (Fig 3-16).

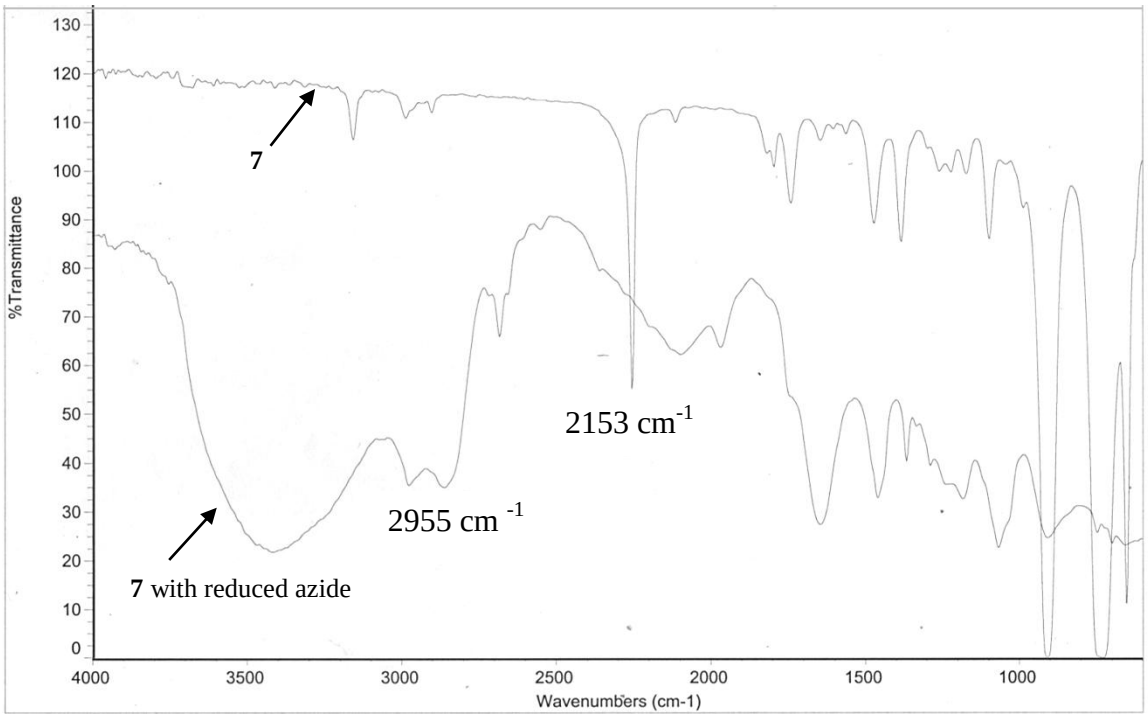


**Figure 3-15:** Infrared spectrum of **7** (top) and **7** with reduced azide (bottom).

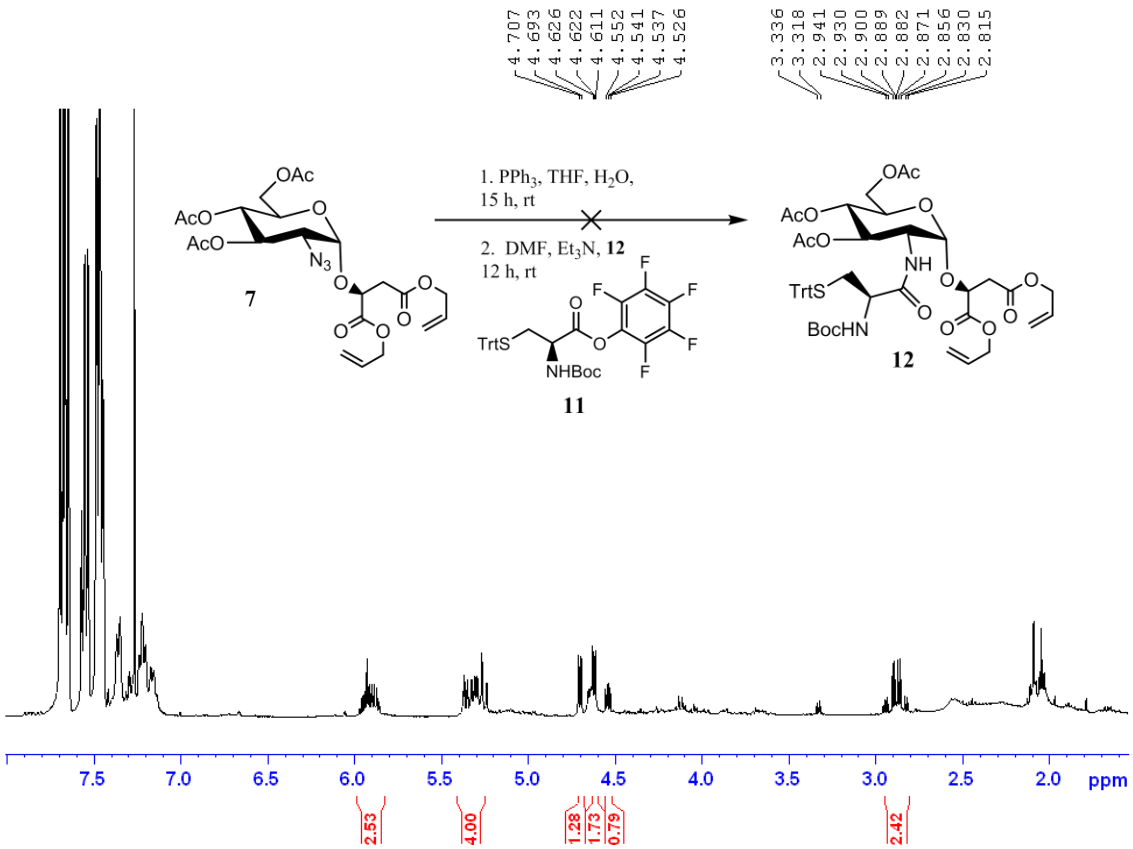


**Figure 3-16:** 400 MHz $^{1}$H NMR of attempted synthesis of cysteinyl diallyl malate ester (**12**) in $CDCl_3$.

Since BSH is known to contribute to fosfomycin resistance in *B. subtilis* an experiment was conducted to determine the minimum concentration of fosfomycin required to inhibit cell growth, or the minimum inhibitory concentration (MIC) (*35*). For this experiment an overnight culture of *B. subtilis* cells were grown at 37 °C in nutrient media. 200 µL of the overnight culture was then plated onto a nutrient media/agar plate. Solutions of fosfomycin (5µL) in varying concentrations were then applied to the paper discs; $H_2O$ was added to one disc as a control. The plate was incubated again overnight at 37 °C. Growth inhibition could be seen as halos around the paper discs where no cell growth was observed. Inhibition was measured as the diameter of the halos in mm. No

inhibition was detected around the $H_2O$ control as expected. Cell growth was only inhibited by fosfomycin concentrations at or above 6.0 mg/mL as seen in table 3-1.

| **Fosfomycin concentration (mg/mL)** | **Diameter of growth inhibition (mm)** |
|---|---|
| $H_2O$ control | None |
| 0.20 | None |
| 0.40 | None |
| 0.60 | None |
| 0.80 | None |
| 1.0 | None |
| 1.2 | None |
| 6.0 | 15.0 |
| 12.0 | 20.0 |
| 24 .0 | 25.0 |
| 60 .0 | 34.0 |
| 120.0 | 38.0 |

**Table 3-1:** Determination of MIC of fosfomycin in *B. subtilis:* measured diameter of inhibiton.

# Chapter 4: Conclusion

Bacillithiol is the major low-molecular-weight thiol in Firmicutes including pathogens *S. aureus*, and *B. anthracis*. BSH has been shown to contribute to resistance to some antibiotics and other stressors in the bacteria that produce it; therefore, full characterization of this LMW thiol should be pursued.

The successful synthesis of a 2-azido-2-deoxy-3,4,6-tri-O-acetyl-α,-D-glucopyranosyl trichloroacetimidate provided a suitable glycosyl donor for the α-anomeric linkage of L-malic acid with D-glucosamine. A diallyl malate ester was synthesized and successfully introduced to the glycosyl donor in the desired α-conformation. A cysteine derivative was activated at the carboxyl group for peptide bond formation with D-glucosamine through the addition of a pentafluorophenyl group. The formation of the peptide bond between D-glucosamine and L-cysteine without the use of a coupling agent was unsuccessful. Disc diffusion assays determined that a minimum fosfomycin concentration of 6 mg/mL is required to inhibit growth in *B. subtilis*.

Future work should include the investigation of peptide coupling reagents for the formation of the peptide bond between D-glucosamine and L-cysteine. This should be followed by removal of the protecting groups to yield BSH. The synthetic BSH should then be used to advance studies of its functions.

# Chapter 5: References


1. Bhave, D.P.; Muse, W.B. III; Carroll, K.S. Drug Targets in Mycobacterial Sulfur Metabolism. *Infectious Disorders-Drug Targets.* **2007**, *7*, 140-158.

2. Fahey, R.C. Novel Thiols of Prokaryotes. *Annu. Rev. Microbiol*. **2001**, *55*, 33-56.

3. Newton, G.L; Fahey, R.C.; Rawat, M. Detoxification of toxins by Bacillithiol in *Staphylococcus aureus*. **2012**, *Microbiology Papers in Press.* Published as doi:10.1099/mic.0.055715-0

4. Winterbourn, C.C.; Metodiewa, D. Reactivity of biologically important thiol compounds with superoxide and hydrogen peroxide. *Free Radical Biology & Medicine.* **1999**, *27*, 323-328.

5. Beinert, H. Iron-sulfur proteins: ancient structures, still full of surprises. *J. Biol. Inorg. Chem.* **2000**, *5*, 2-15.

6. Fahey, R.C.; Buschbacher, R.M.; Newton, G.L. The Evolution of Glutathione Metabolism in Phototrophic Microorganisms. *J. Mol. Evol.* **1987**, *25*, 81-88**.**

**7.** Dickinson, D.; Forman, H.J. Cellular glutathione and thiols in metabolism. *Biochem. Pharmacol.* **2002**, *64*, 1019-1026.

8. Götz, M.; Künig, G.; Reiderer, P.; Youdim, M.B.H. Oxidative Stress: Free Radical Production in Neural Degeneration. *Pharmac. Ther.* **1994**, *63*, 37-122.

9. Matés, J.M.; Pérez-Gómez, C.; Núñez De Castro, I. Antioxidant Enzymes and Human Diseases. *Clinical Biochemistry*. **1999**, *32*, 595-603.

10. Forman, H.J.; Zhang, H.; Rinna, A. Glutathione: Overveiw of its protective roles, measurement, and biosynthesis. *Mol. Aspects Med.* **2009**, *30*, 1-12.

11. Foote, N.; Turner, R.; Brittain, T.; Greenwood, C. A quantitative model for the mechanism of action of the cytochrome *c* peroxidase of *Pseudomonas aeruginosa*. *Eur. J. Biochem.* **1995**, *230*, 821-825.

12. Chi, B.K.; Gronau, K.; Mäder, U.; Hessling, B.; Dörte, B.; Antelmann, H. S-bacillithiolation rotects against hypochlorite stress in *Bacillus subtilis* as revealed by transcriptomics and redox proteomics. *Mol. Cell Proteomics.* **2011**, *10*, M111.009506.

13. Haddad, J.J.; Harb, H.L. L-γ-Glutamyl-L-cysteinyl-glycine (glutathione; GSH) and GSH related enzymes in the regulation of pro- and anti-inflammatory cytokines: a signaling transcriptional scenario for redox(y) immunologic sensor(s)? *Mol. Immunol*. **2005**, *42*, 987-1014.

14. Monostori, P.; Wittman, G.; Karg, E.; Turi, S. Determination of glutathione and glutathione disulfide in biological samples: An in-depth review. *J. Chromatogr., B: Anal. Technol. Biomed. Life Sci.* **2009**, *877*, 3331-3346.

15. Biterova, E.I.; Barycki, J.J. Mechanistic details of glutathione biosynthesis revealed by crystal structures of *Saccharomyces cerevisiae* glutamate cysteine ligase. *J Biol Chem.* **2009**, *284*, 32700-32708.

16. Newton, G.L.; Leung, S.S.; Wakabayashi, J.I.; Rawat, M.; Fahey, R.C. The DinB Superfamily includes Novel Mycothiol, Bacillithiol, and Glutathione S-transferases. *Biochemistry*. **2011**, *50*, 10751-10760.

17. Oakly, A.J.; Rossjohn, J.; Lo Bello, M.; Caccrui, A.M.; Federici, G.; Parker, M.W. The Three Dimensional Structure of the Human Pi Class glutathione Transferase P1-1 in Complex with inhibitor Ethacrynic Acid and Its Conjugate. *Biochemistry*. **1997**, *36*, 576-585.

18. Newton, G.L.; Buchmeier, N.; Fahey, R.C. Biosynthesis and functions of mycothiol, the unique protective thiol of *Actinobacteria. Microbiol. Mol. Biol. Rev.* **2008**. *72*, 471-494.

19. Rawat, M.; Av-Gay, Y. Mycothiol-dependent proteins in actinomycetes. *FEMS Microbiol. Rev.* 2007, *31*, 278-292.

20. Newton, G.L. Bacillithiol is an antioxidant thiol produced in Bacilli. *Nat.Chem. Biol*. **2009**, *5*, 625-627.

21. Gaballa, A.; Newton, G.L.; Antelmann, H.; Parsonage, D.; Upton, H.; Rawat, M.; Claibrone, A.; Fahey, R.C.; Helmann, J.D. Biosynthesis and functions of bacillithiol, a major low-molecular-weight thiol in Bacilli. *PNAS*. **2010**, *107*, 6482-6486.

22. Parsonage, D.; Newton, G.L.; Holder, R.C.; Wallace, B.D.; Paige, C.; Hamilton, C.J.; Dos Santos, P.C.; Redinbo, M.R.; Reid, S.D.; Claiborne, A. Characterization of *N*-Acetyl-α-D-glucosaminyl L-Malate Synthase and Deacetylase Functions for Bacillithiol Biosynthesis in *Bacillus anthracis*. *Biochemistry*. **2010**, *49*, 8398-8414.

23. Zoelby, A. E.; Sansschragin, F.; Levesque, R. C. Structure and function of the Mur enzymes: development of novel inhibitors. *Molec. Microbiol.* **2033**, *47*, 1-12.

24. Helmann, John D. Bacillithiol, a New Player in Bacterial Redox Homeostasis. *Antioxid. Redox Signaling*. **2011**, *15*, 123-133.

25. Sharma, S.V.; Jothivasan, V.K.; Newton, G.L.; Upton, H.; Wakabayashi, J.I.; Kane, M.G.; Roberts, A.A.; Rawat, M.; La Clair, J.J.; and Hamilton, C.J. Chemical and Chemoenzymatic Synthesis of Bacillithiol: A unique Low-Molecular-Weight Thiol amongst Low G + C Gram Positive Bacteria. *Angew. Chem., Int. Ed*. **2011**, *50*, 7101-7104.

26. Stewart, M.J.G.; Jothivasan, V.K.; Rowan, A.S.; Wagg, J.; Hamilton, C.J. Mycothiol disulfide reductase: solid phase synthesis and evaluation of alternative substrate analogues. *Org. Biomol. Chem.* **2008**, *6*, 385-390.

27. Patel, M.P.; Blanchard, J.S. Synthesis of Des-*myo*-Inositol Mycothiol and Demonstration of a Mycobacterial Specific Reductase Activity. *J. Am. Chem. Soc.* **1998**, *120*, 11538-11539.

28. Lee, S.; Rosazza, J.P.N. First Total Synthesis of Mycothiol and Mycothiol Disulfide. *Org Lett.* **2004**, *6*, 365-368.

29. Demchenko, A. V. General Aspects of the Glycosidic Bond Formation, in Handbook of Chemical Glycosylation: Advances in Stereoselectivity and Therapeutic Relevance (ed A. V. Demchenko), Wiley-VCH Verlag GmbH & Co. **2008.** doi: 10.1002/9783527621644.ch1

30. Juaristi, E.; Cuevas, G. Recent studies of the anomeric effect. *Tetrahedron*. **1992**, *24*, 5019-5087.

31. Han, S.; Kim, Y. Recent development of peptide coupling reagents in organic synthesis. *Tetrahedron.* **2004**, *60*, 2447-2467.

32. Rele, S. M.; Iyer, S. S.; Baskaran, S.; Chaikof, E.L.; Design and synthesis of dimeric heparinoid mimetics. *J. Org. Chem.* **2004**, *69*, 9159-9170.

33. Pennington, M. W.; Byrnes, M. E.; Procedures to improve difficult couplings: Peptide Synthesis Protocols. *Meth. Mol. Biol*. **1994**, *35*.

34. Jenson, C. M.; Lee, D. Dry Ice Bath Based on Ethylene Glycol mixtures. *J. Chem. Educ.* **2000**, *77*, 629.

35. Andrews, J. M. Determination of minimum inhibitory concentrations. *J. Antimicrob. Chemoth.* **2001**, *48*, 5-16.